

Check for updates

# **Bioinspired Design of Heterogenous Single-Atomic-Site Catalysts for Electrocatalysis and Photocatalysis**

Ying Wang, Guangri Jia, Piaoping Yang,\* Linshan Zhang, and Kwok-Yin Wong\*

The emergence of single-atomic-site catalysts (SACs) provides a specific model to bridge the gap between homogeneous and heterogeneous catalysis. An interesting aspect in SACs is how to apply the bioinspired strategies in homogeneous biocatalysis to the design of heterogeneous SACs. The effectiveness of this approach relies on systematic insights in structural characteristics and catalytic mechanisms of both the biocatalysts and the heterogeneous SACs. This review will give a summary on the representative bioinspired single-atomic-site catalysts and their applications in heterogeneous electrocatalysis and photocatalysis. The fundamentals of bioinspired design strategies will be systematically discussed in the first shell coordination (quasi-homogeneous metal centers and coordination numbers/species) and the second/long-range coordination (heteroatoms doping, dual-metallic sites, nano-single-atom-site, and metal-support interaction). Also, the unique non-covalent interactions and oriented mass/proton/electron transfer channels in heterogenous SACs are highlighted as inspired by the outer microenvironment of biological systems. The practical electrocatalytic and photocatalytic applications of bioinspired SACs are further discussed by drawing inspiration from hydrogenase, nitrogenase, oxidase, and dehydrogenase to produce hydrogen-, carbon-, nitrogen-, and oxygen-based value-added chemicals. The current challenges and future opportunities for the development of bioinspired heterogenous SACs will also be discussed.

1. Introduction

Sustainable energy and the global environment are essential considerations when we promote carbon-neutral energy transformation to achieve an eco-friendly development in modern human society.<sup>[1,2]</sup> In modern industrial processes, catalysis stands

as one of the most transformative scientific advancements, underpinning numerous sectors and driving unparalleled development and innovation. Catalysis, the process of accelerating chemical reactions using a substance (the catalyst) which itself remains unchanged, has profound implications for the efficiency, sustainability, and economic viability of industrial processes. Electro-/photocatalysis hold great promise for substituting conventionally heat-driven catalysis and fulfilling the requirement of sustainable development.[3,4] The pursuit of economic and efficient electro-/photocatalysts has become a scientific prerequisite for wide practical applications. Specifically, the stability and easy recovery of heterogeneous catalysts make them viable alternatives to homogeneous catalysts and biological (enzyme) catalysts.<sup>[5]</sup> Conventional heterogeneous electro-/photocatalysts are typically composed of multiple aggregated metal atoms with different properties.[6,7] The insufficient metal utilization efficiency and complicated catalytic process are the major intrinsic fragility hindering widespread adoption.

To fully harness atomic economy, single-atom-site catalysts (SACs) have emerged as a promising frontier in the field of heterogeneous catalysis.<sup>[8]</sup> SACs feature well-defined coordination geometry and much higher atom-utilization efficiency compared to their nanoparticle and bulk counterparts.<sup>[9,10]</sup> These intriguing properties make SACs potential candidates to bridge

Y. Wang, L. Zhang, K.-Y. Wong State Key Laboratory of Chemical Biology and Drug Discovery Department of Applied Biology and Chemical Technology The Hong Kong Polytechnic University Hung Hom, Kowloon, Hong Kong SAR, China E-mail: kwok-yin.wong@polyu.edu.hk

The ORCID identification number(s) for the author(s) of this article can be found under https://doi.org/10.1002/adma.202502131

© 2025 The Author(s). Advanced Materials published by Wiley-VCH GmbH. This is an open access article under the terms of the Creative Commons Attribution-NonCommercial-NoDerivs License, which permits use and distribution in any medium, provided the original work is properly cited, the use is non-commercial and no modifications or adaptations are made.

DOI: 10.1002/adma.202502131

Y. Wang, P. Yang

Key Laboratory of Superlight Materials and Surface Technology Ministry of Education College of Materials Science and Chemical Engineering

Harbin Engineering University Harbin 150001, P. R. China

E-mail: yangpiaoping@hrbeu.edu.cn

G. Jia

Department of Chemistry The University of Hong Kong Pokfulam Road, Hong Kong SAR, China



ADVANCED MATERIALS

they are still in their infant stage, and timely and systematic summaries focusing on bioinspired engineering approaches of SACs-based catalysts, reactions, and devices would greatly benefit the researchers working in this area.

the gap between heterogeneous and homogeneous catalysis.<sup>[11]</sup> Additionally, SACs provide an ideal model for demonstrating the structure-property-performance relationships in various electro-/photocatalytic reactions. Over the past decade, SACs have garnered enthusiastic attention in both scientific research and industrial applications for energy-related electro-/photocatalysis.[12-14] For instance, Zeng et al. provided a detailed review on SACs for various electrochemical clean energy reactions, such as water splitting and fuel cells, as well as green chemistry applications like ammonia synthesis and carbon dioxide reduction (CO2RR).[15] Xiong's group conducted a comprehensive summary on single-atom photocatalysts for sustainable energy conversion, organic synthesis, and environmental remediation.[16] These timely reviews reflect that SACs have attracted intense attention as potential catalysts for energy-related chemical processes.

In this review, we aim to present state-of-the-art research, summarize fundamental principles, and discuss the rational design of more efficient bioinspired SACs for heterogeneous electro-/photocatalytic reactions. We will start with a brief description on the development of versatile fabrication strategies for SACs, emphasizing the functional concept of bioinspired strategies across all scales. Following this, we will discuss the bioinspired principles for engineering the first shell coordination (quasi-homogeneous metal centers, coordination numbers, and coordination species), the second /long-range coordination (heteroatom doping, dual-metallic sites, nano-single-atomsite, and metal-support interaction), and the outer microenvironment (noncovalent interaction and mass/proton/electron transfer) of heterogeneous SACs. To elaborate these emerging developments, SACs inspired from hydrogenase, nitrogenase, oxidase, and dehydrogenase in different electro-/photocatalytic reactions to produce hydrogen-, carbon-, nitrogen-, and oxygenbased value-added chemicals are highlighted. Finally, we will discuss the existing challenges and give a comprehensive perspective on these bioinspired SACs for heterogeneous electro-/photocatalysis (Figure 1).

The ultimate goal of catalysis research is to achieve feasible applications for the industries. In this context, the pursuit of low-cost, large-scale, and high-efficiency single-atomsite catalysts (SACs) is crucial for the successful implementation of green energy conversion technologies.[17] The development of well-defined SACs primarily relies on typical design principles, including size, electronic structure, and coordination environment.[18,19] Traditional SACs are primarily geometric homologues of their homogeneous counterparts, despite being heterogeneous in nature. Maximizing metal atom dispersion on supports (e.g., oxides, carbons) is a challenge to fabricate traditional SACs for diverse applications. Moreover, there is limited control over the geometric structure and electronic properties of the ligands. The coordination environment is often inadequate and usually depends on the inherent properties of the ligands and supports.

## 2. Bioinspired Design for Engineering Heterogeneous SACs Structures

Natural enzymes are highly regarded as the pinnacle of homogeneous biocatalysts due to their intrinsic activity and selectivity.<sup>[20]</sup> Reflecting on the journey of single-atomic-site catalysts (SACs), the development of state-of-the-art SACs has drawn inspiration from natural biological systems. Nature provides blueprints for the effective utilization and artificial biocatalysis of sustainable energy conversion in biological organisms.<sup>[21]</sup> Most importantly, the intrinsically scaling and hierarchical structures in natural biocatalytic systems offer vast opportunities for energy device design methodology. The concept of natureinspired chemical engineering has been successfully proposed and implemented into bioinspired sustainable nanomaterials and devices.[22,23] Embracing these bioinspired strategies in the rational design of heterogeneous SACs promises breakthroughs in key energy conversion reactions. For bioinspired SACs, researchers need to mimic the active sites of metalloenzymes by replicating their coordination environments. These catalysts often feature precise ligand arrangements (e.g., N, S, O ligands) and secondary coordination spheres that stabilize reaction intermediates or facilitate specific reaction pathways. In essence, bioinspired SACs integrate principles from natural catalysis to achieve superior specificity and efficiency in targeted reactions, while traditional SACs focus on dispersion of catalytic sites and stability for different applications. The former bridges the gap between enzymatic and industrial catalysis, whereas the latter focuses on scalable and robust material design. Although natureinspired heterogeneous SACs have emerged in recent literature,

The exploration of practical design strategies and fabrication methods for single-atom-site catalysts (SACs) at the atomic level is crucial for industrial energy conversion. Previous studies have confirmed that the physical and chemical properties of SACs can be precisely tuned by carefully modifying the coordination configuration and local microenvironment.[24-26] Recent advances in synthetic strategies and characterization tools have significantly advanced the design of single-atomic-site catalysts. Synthesis methods can be broadly categorized as topdown or bottom-up approaches. In the top-down approach, the bulk materials are broken down into isolated atoms by thermochemical treatments such as high-temperature etching or physical processes like ball milling, [27,28] microwave, and laser irradiation.[29,30] While these methods are cost-effective and scalable, they often lack precise control over atomic dispersion.[31] In contrast, bottom-up strategies anchor single atoms onto tailored supports via wet-chemical synthesis, [32] pyrolysis-assisted stabilization,[33,34] or defect engineering.[35] These methods enable precise control over active site density, coordination environment, and scalability. To establish the structure-activity relationship of SACs, advanced characterization techniques are essential. Table 1 summarizes the various characterization techniques for SACs. Atomic-resolved high-angle annular dark field scanning transmission electron microscopy (HAADF-STEM) combined with electron energy loss spectroscopy (EELS) directly visualizes isolated atoms, while X-ray photoelectron spectroscopy (XPS) and synchrotron X-ray absorption spectroscopy (XAS) provide information on the chemical states and coordination environments.[36,37] However, to capture dynamic structural changes under reaction conditions, in situ XAS and

wiley.com/doi/10.1002/adma.202502131 by HONG KONG POLYTECHNIC UNIVERSITY HU NG HOM, Wiley Online Library on [28:09/2025]. See the Terms

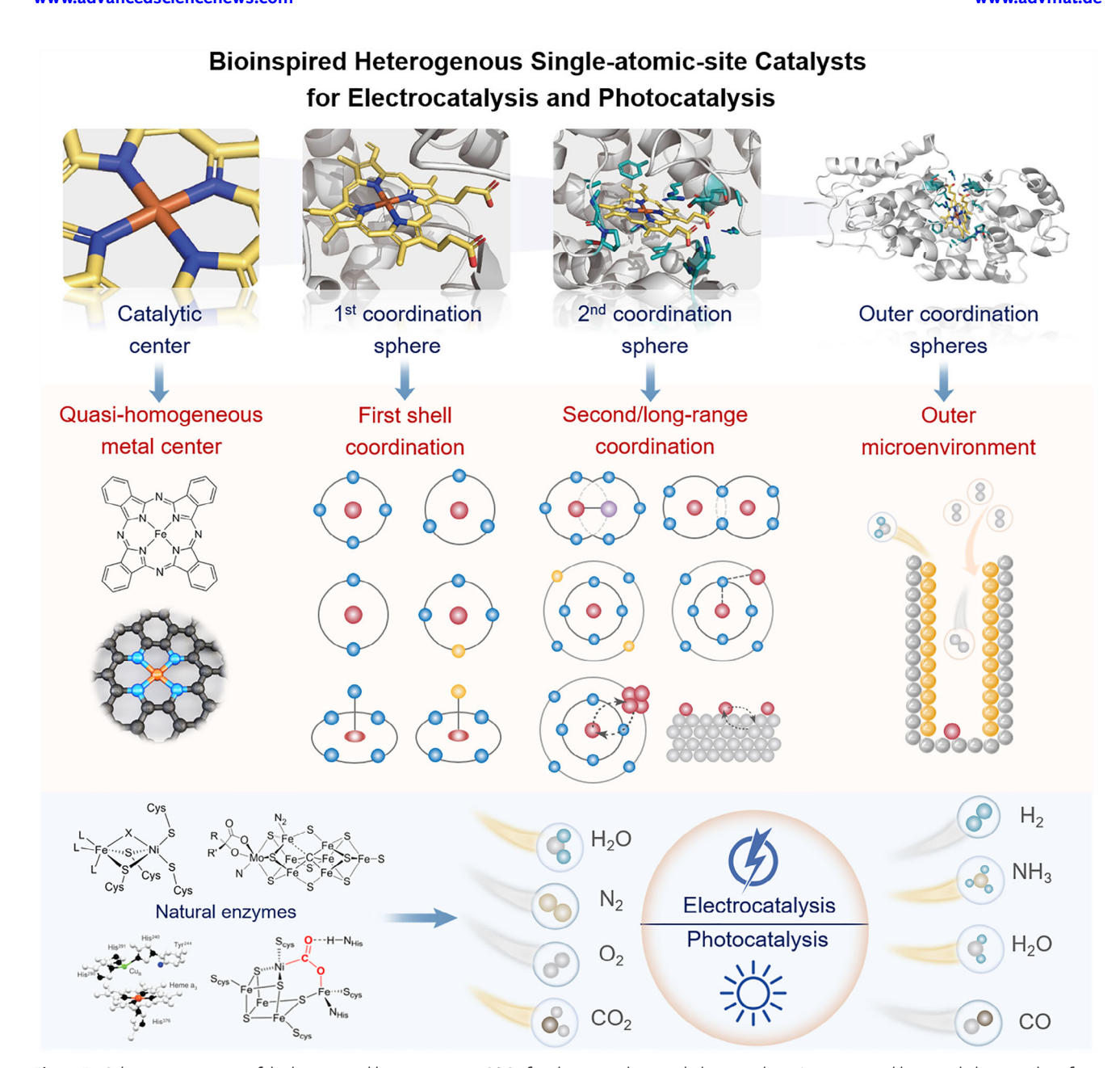


Figure 1. Schematic overview of the bioinspired heterogeneous SACs for electrocatalysis and photocatalysis (inset: natural horseradish peroxidase from PDB entry 1HCH).

**Table 1.** The summary of advanced characterization for single atom.

Characterization	Role/Function	Structure-Activity Relationship	Scale
HAADF-STEM	Morphology	Single atom sites	Local position
EELS	Element validation	Element type and valence state	Local position
XPS	Chemical state	Valence state and surface content of Single atom	Surface position
XAS	Coordination environment	Single atom environment	Bulk
In situ FTIR	Functional group	Intermediate tracking	Surface position
In situ XAS	Coordination environment evolution	Active site evolution	Bulk

www.advmat.de

15214095, 0, Downloaded from https://advanced.onlinelibrary.wiley.com/doi/10.1002/adma.202502131 by HONG KONG POLYTECHNIC UNIVERSITY HUNG HOM, Wiley Online Library on [28.09/2025]. See the Terms and Conditions (https://onlinelibrary.wiley.

and-conditions) on Wiley Online Library for rules of use; OA articles are governed by the applicable Creative Commons

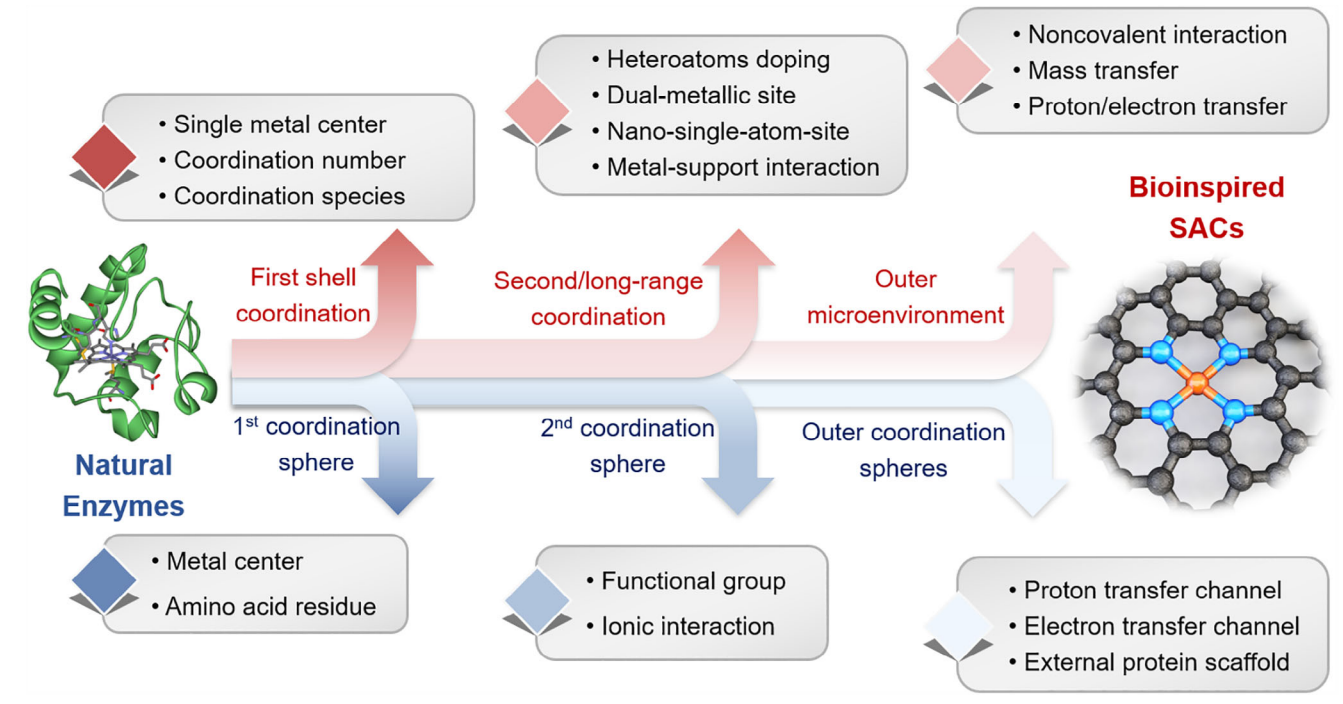


Figure 2. Schematic illustration of the bioinspired engineering strategies for heterogeneous SACs structures (PDB entry 1HCH).

infrared spectroscopy are indispensable, revealing real-time evolution during catalysis.[38,39]

The most promising source of inspiration for designing and engineering heterogeneous SACs structures are metalloenzymes in biological organisms. Every component and scaffold in metalloenzymes have evolved elaborately over millions of years and underpin an indispensable part in biocatalytic processes. Therefore, the crucial principle for designing bioinspired SACs is to embrace both the structural and functional characteristics integrally rather than merely copying seemingly useful features within enzymes.<sup>[40]</sup> As illustrated in Figure 2, the structure of metalloenzymes mainly consists of the active metal centers and peptide matrix in coordination spheres. Specifically, the corresponding protein scaffold in metalloenzymes can be further systematically categorized into three separate regions beyond the active sites: (1) The first coordination sphere comprises of atoms or amino acid residues that are linked with the central metal; (2) The second coordination sphere incorporates the functional groups with ionic interactions close to the metal center; (3) The outer microenvironment with defined proton and electron transfer channels composed of the remaining external protein scaffold, solvent, and ions.[41,42] It is possible that these features of natural enzymes can be well grafted into the rational bioinspired design of heterogeneous SACs. Accordingly, this section will give an overview of the general bioinspired principles for engineering metal centers with precise coordination number/species in the first shell coordination, as well as the synergistic effect of heteroatoms, neighboring metallic sites, nanoparticles and supports in the second/long-range coordination with the metal active centers of heterogeneous SACs. The noncovalent interaction and mass/proton/electron transfer in the outer microenvironment as inspired by the biological systems will also be discussed.

## 2.1. Bioinspired Engineering of the First Shell Coordination of SACs

The intrinsic catalytic properties of SACs are primarily associated with the isolated metal centers anchored on concomitant supports with precise configuration. Moreover, the electronic properties (e.g., valence state, spin state, electron density near Fermi level (EF)) of isolated central metal sites can be well mediated by the diversity of coordination in SACs.<sup>[43]</sup> The cation metal center is covalently bonded with proximal atoms and accompanied by direct charge transfer in the first-coordination of SACs configuration, which possesses close similarities to their homogeneous enzyme scaffold analogues in the first coordination sphere. The bioinspired design of quasi-homogeneous metal centers, coordination numbers, and coordination species on the atomic scale offer us fascinating strategies to further elevate the geometric and electronic structures for state-of-the-art SACs.

### 2.1.1. Bioinspired Design of Quasi-homogeneous Metal Center for SACs

Hitherto, numerous approaches in SACs synthetic strategies have been developed to atomically disperse most metal atoms across the periodic table onto various supports. [44] Based on the Sabatier principle, the optimal heterogeneous catalysis requires binding energy of intermediate strength between catalysts and substrates. [45] Therefore, transition metals are the main elemental scopes of SACs by virtue of their unfilled *d* electron orbitals. A number of noble metals-based SACs (e.g., Au, Pd, Pt, Ir, and Ru) have displayed remarkable performance in various electro/photo-catalytic processes. [46,47] To further meet the requirement



ADVANCED MATERIALS

www.advmat.de

of practical applications, non-noble metal-based SACs are highly desirable to lower the fabrication costs in practical devices. [48] Many metalloenzymes are composed of non-noble metals in the active sites, which are analogous to the isolated atom sites in SACs. The initial attempts to mimic the complex enzymic framework are mainly focused on mimicking the configurations of active centers in enzymes. In this case, strategies on mimicking the homogeneous non-noble metal centers in enzymes for SACs appear to be an efficient approach to improve heterogenous catalytic performance.

Porphyrins are cyclic tetrapyrrolic macromolecules composed of four pyrrole subunits with methylene bridges, which can bind with various transition metals and main group elements (Figure 3a). In nature, metalloporphyrins play significant roles in many biological systems and processes. [49] For example, the heme group, a kind of iron-containing metalloporphyrin, is involved in a wide range of biological oxygen binding, transport, and storage. [50] Chlorophyll is a magnesium-containing metalloporphyrin, and is a key component for photosynthesis in plants and algae. From a structural aspect, the configuration of those metalloporphyrins is closely similar to the square-planar M-N<sub>4</sub> coordination center in heterogenous SACs geometry, which is ideal for substrate binding and activation in electro-/photocatalytic reaction processes.<sup>[51]</sup> Numerous studies have demonstrated that those structural analogues of metalloporphyrins can stabilize metal ions of various oxidation states, thereby enhancing the performance of important reactions such as oxygen reduction reaction (ORR), hydrogen evolution reaction (HER), and oxygen evolution reaction (OER) (Figure 3b).[52]

Phthalocyanines (Pcs) consist of four isoindole subunits with 18 p-electrons and possess structural similarity to naturally occurring porphyrins (Figure 3c). [53] Different transition metals can be coordinated in the center of the phthalocyanine ring to form a series of metallophthalocyanines with unique catalytic properties. Specifically, iron phthalocyanines (FePc) with promising ORR catalytic activity has been regarded as one of the most promising candidates to replace the expensive Pt-based catalysts.[54] Pioneering work has demonstrated that cobalt phthalocyanine (CoPc) can be developed as CO<sub>2</sub> reduction reaction (CO<sub>2</sub>RR) catalyst to mediate CO<sub>2</sub>-to-CO conversion. [55] Additionally, Liang and coworkercoworkers have presented a series of nickel phthalocyanine (NiPc) molecules multi-walled carbon nanotubes (CNTs) as molecularly dispersed electrocatalysts (MDEs).[56] The optimized MDEs can afford the conversion of CO2 to CO with >99.5% selectivity at -150 mA cm<sup>-2</sup> and 0.50 V overpotential for 40 h in a gas diffusion electrode (GDE) device. Wang and colleagues meticulously have engineered CoPc molecules highly dispersed on highly conductive carbon nanotubes via noncovalent anchoring strategy (Figure 3d).<sup>[57]</sup> Interestingly, this improved moleculebased electrocatalyst can achieve the impressive six-electron reduction of CO2 to methanol with CO intermediates via a distinct domino process.

Under those appreciable pioneering results of homogenous metal-macrocycle derivatives, multiple  $M-N_4/C$  active sites are further successfully designed and constructed in heterogenous SACs for various small molecule activation processes. Inspired by the coordination structure of Fe-based peroxidase, Cheng's group have designed a ferriporphyrin-based network with a monatomic Fe- $N_4$  coordination center as dual-functional ar-

tificial peroxidase (Figure 3e).<sup>[58]</sup> Shi et al. also use similar biomimetic synthetic strategy for the facile preparation of atomically dispersed iron single-atom catalysts with Fe-N<sub>4</sub>O<sub>2</sub> structure (Figure 3f). [59] Additionally, this typical bioinspired singleatom Fe site is further employed in photo-Fenton-like reactions. For example, Wu and coworkercoworkers have constructed bioinspired SACs by embedding pyrrole-type FeN<sub>4</sub> sites in graphitic carbon nitride (g-C<sub>2</sub>N<sub>4</sub>) by facile copolymerization procedures (bio-SA-Fe/g-C<sub>3</sub>N<sub>4</sub>), leading to excellent photocatalytic Fenton performance. [60] Apart from Fe active sites, copper ions in enzymes also play crucial roles in facilitating the metabolism of oxygen and nitrogen compounds. By mimicking the electronic and structural characteristics of natural Cu superoxide dismutase (SOD), Yan and colleagues have successfully prepared atomically dispersed Cu-N<sub>4</sub> sites in heterogenous SACs via a carbonization process (Figure 3g).<sup>[61]</sup> Similar to the configuration of multiple copper ions in natural laccases, Gazit et al. have investigated the redox-active divalent copper ions (Cu<sup>2+</sup>) in ultrathin 2D layered structures by supramolecular assembly of single amino acid phenylalanine. This as-constructed Cu-based catalyst can facilitate the catalytic oxidation of phenolic contaminates similar to the laccase enzyme. [62] In another study, Xia and colleagues have proposed an effective approach to construct active copper nanocomposites (CPG-900) via mimicking the catalytic sites in natural cytochrome c oxidase and laccase. The resulting CPG-900 exhibits excellent electrocatalytic oxygen reduction/evolution performance at closely approaching standard potentials by virtue of the optimal environment for electronic bonding of O2 to Cu2+ ions. [63] Furthermore, magnesium is one of the most abundant cations in cells to facilitate a wide variety of enzymatic reactions. Remarkably, Xie et al. present a highly stable artificial chlorophyll-like Mg−NC structure to mimic the Mg−N<sub>4</sub>-centered chlorophyll units in chloroplasts of natural leaves (Figure 3h).[64] The plentiful Mg-N<sub>4</sub> active centers in the SACs nanostructures play essential roles as electronic donors, thus improving the photocatalytic CO2 cycloaddition performance. Chen and coworkercoworkers have developed Mn active sites atomically dispersed on graphene frameworks to mimic the manganese-containing enzymes. [65] The well-defined Mn-N<sub>3</sub>O<sub>1</sub> cofactor enables the impressive electrocatalytic ORR properties with a relative low onset potential and superior performance for a zinc-air battery device. Additionally, to capitalize on the inspiration of natural enzymes adequately, Ye and her colleagues have reported a series of transition metal single-atoms loaded into graphyne carriers (Figure 3i). [66] The bioinspired incorporation of well-defined metal single-atoms of Fe, Mn, and Mo active centers with reliable coordination and dispersion environment introduce a feasible pathway for designing heterogenous SACs.

#### 2.1.2. Bioinspired Regulation of Coordination Numbers for SACs

The active moieties in heterogenous SACs not only consist of atomically isolated metal centers, but also the surrounding nonmetal atoms coordinated to the cation metal sites directly. As discussed in the above section, the phthalocyanine-like  $M\!-\!N_4$  planar configuration is the most commonly classic and stable coordination structure in heterogenous SACs. Even so, the metal site is in the same plane under saturated electronic conditions, leading

15214095, 0, Downloaded from https://advanced.onlinelibrary.wiley.com/doi/10.1002/adma.202502131 by HONG KONG POL YTECHNIC UNIVERSITY HU NG HOM, Wiley Online Library on [28/09/2025]. See the Terms

and-conditions) on Wiley Online Library for rules of use; OA articles are governed by the applicable Creative Commons

#### Metallomacrocycles

#### Quasi-homogeneous Metal Center

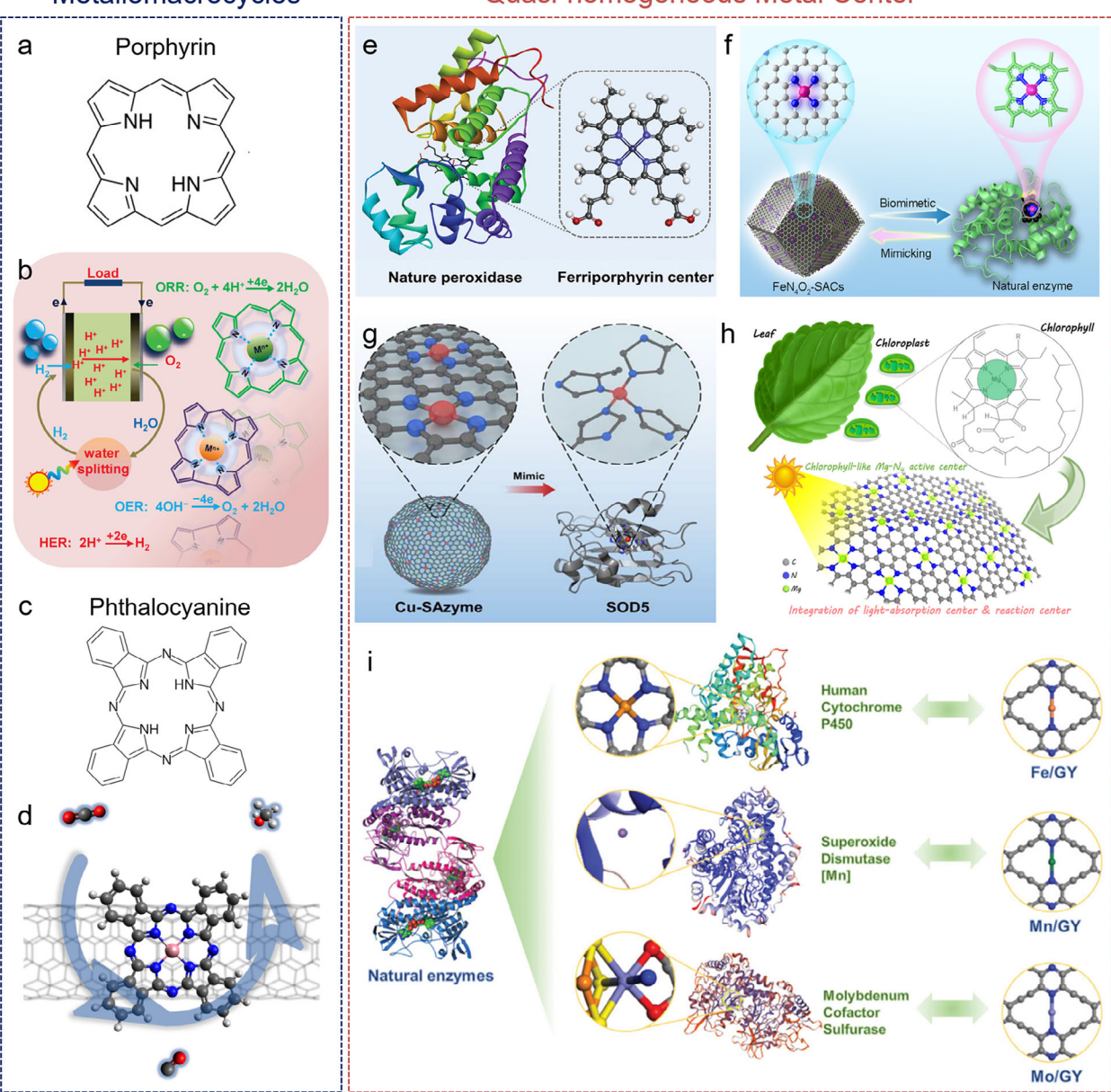


Figure 3. a) Molecular structure of porphyrins. b) Schematic diagram of porphyrin- and corrole-based catalysts for enhancing the efficiency of hydrogen evolution, oxygen evolution, and oxygen reduction reactions. Reproduced with permission. [52] Copyright 2016, American Chemical Society. c) Molecular structure of phthalocyanines. d) Domino process for converting CO2 to MeOH through CO, catalyzed by CoPc on carbon nanotubes (CNTs). Reproduced with permission. [57] Copyright 2019, Springer Nature. e) Biomimetic design of ferriporphyrin networks. Adapted with permission. [58] Copyright 2023, Wiley-VCH. f) Synthesis method for biomimetic FeN<sub>4</sub>O<sub>2</sub>-SACs. Adapted under the terms of the CC-BY Creative Commons Attribution 4.0 International License. [59] Copyright 2023, The Author(s), Springer Nature. g) Schematic depiction of the synthesis of Cu-SAzyme. Adapted under the terms of the CC-BY Creative Commons Attribution 4.0 International License. [61] Copyright 2022, The Author(s), John Wiley and Sons. h) Schematic depiction of a chlorophyll-inspired Mg-NC structure, modeled after the microarchitecture of natural leaves. Reproduced under the terms of the CC-BY Creative Commons Attribution 3.0 Unported License [64] This figure has been published in CCS Chemistry 2024; Artificial Chlorophyll-like Structure for Photocatalytic CO<sub>2</sub> Chemical Fixation is available online at https://doi.org/10.31635/ccschem.024.202404189. i) The design for synthesizing and structuring Fe/GY, Mn/GY, and Mo/GY is influenced by natural enzymes. Reproduced with permission. [66] Copyright 2024, Wiley-VCH.

to limited optimized reactant/intermediate ad-/desorption energies and hindering the overall electro-/photo-catalytic reaction kinetics. Developing advanced coordination engineering strategies is essential for preparing SACs with improved catalytic performance. In this case, nature-inspired engineering methodology becomes another efficient approach to precisely regulate the coordination number for constructing bioimitating SACs.

Given that flexible modulation of the local environment of metal sites in SACs is restricted by the stable rigid construction with four proximal N sites, the breaking of the centro-symmetry

#### **Bioinspired Regulation of Coordination Numbers**

## In-plane regulation of coordination numbers Axial regulation of coordination numbers M-N In-plane M-N<sub>4</sub> Anodic ECL е TMR TMR Fe-N. site in a Fe-N-C catalys globin and a synthetic model

Figure 4. a) Diagram illustrating the synthesis approach for CuN₂-SAzyme and CuN₄-SAzyme. Adapted under the terms of the CC-BY Creative Commons Attribution 4.0 International License. [69] Copyright 2024, The Author(s), Springer Nature. b) Diagram illustrating of the detection outcomes of pFeSAN based on a biomimetic synthetic strategy. Adapted under the terms of the CC-BY Creative Commons Attribution 4.0 International License. [70] Copyright 2023, The Author(s), Springer Nature. c) Diagram of the synthesis of carbon nanoframe with atomically dispersed Fe sites in five-N axial coordination. Adapted with permission. [72] Copyright 2019, the American Association for the Advancement of Science. d) Schematic diagram of bioinspired single-atom sites with FeNs axial coordination for switching anodic/cathodic electrochemiluminescence (ECL). Adapted with permission. [73] Copyright 2023, Wiley-VCH. e) The atomically dispersed Fe-N-C catalyst and its associated metalloprotein. Left panel (single-atom catalyst): Adapted with permission. [74] Copyright 2017, American Chemical Society. Right panel (metalloprotein): Adapted with permission. [75] Copyright 2018, Springer Nature. f) The Ni-N active sites in different natural enzyme and nanozyme frameworks. Reproduced with permission. [76] Copyright 2022, Wiley-VCH.

of the M-N<sub>4</sub> structure is of critical importance. Recent studies have validated that tuning the number of coordination atoms provides a viable approach to modify the electronic structure of the atomic metal center.<sup>[25,67,68]</sup> In addition, enzymatic function can be altered by adjusting the amnio acid residues coordinated with the metal ions in natural enzymes. Specifically, Li and coworkers have created a CuN3-centered SACs via local coordination manipulation for enhancing radio-enzymatic therapy (Figure 4a). [69] It was observed that reducing the coordinated number of nitrogen atoms could protrude the CuN3 active moiety from the carbon plane, thereby presenting higher optimal H<sub>2</sub>O<sub>2</sub> substrate adsorption/dissociation than a planar CuN<sub>4</sub>-centered counterpart. Besides the above saturated coordination, decreasing the coordination number of central metals can also lead to unsaturated coordination with defect or vacancy sites on the SACs substrate. Inspired by the structure of natural metalloenzymes, Qu's group has proposed a biomimetic synthetic strategy to build atomically dispersed Fe sites with Fe-N3 coordination (Figure 4b).<sup>[70]</sup> Impressively, this as-constructed Fe-N<sub>3</sub> moiety with abundant N defect sites facilitates strong oxygen adsorption/activation, thereby affecting the complete oxygen-towater oxidation pathway similar to natural cytochrome c oxidase (CcO).

Apart from low coordination design, isolated metal centers in oversaturated SAC structures have also been established to disrupt the electronic balance in saturated M-N<sub>4</sub> configuration with impressive properties.<sup>[71]</sup> The corresponding inspiration can be derived from the amino acid residues (e.g., histidine (His) or methionine) as natural enzyme ligands in an axial position. Advantageously, the introduction of additional axial ligand in the M-N<sub>4</sub> coordination can increase the electropositivity of central metal sites with unique asymmetric electron distribution. As a typical example, Dong and coworkers have constructed a confined axial N-coordinated FeN<sub>5</sub> atomic active centers in the carbon nanoframe (FeN5 SA/CNF) through mimicking the spatial structure of axial-coordinated hemes of oxidoreductases (Figure 4c).<sup>[72]</sup> The as-synthesized axial N coordination in FeN5 SA/CNF catalyst plays a key role in driving the oxidase-like push effect and electron donation mechanism. Additionally, inspired by the skyscraping selectivity of natural enzymes, Zhu and coworkercoworkers also assemble the well-defined FeN<sub>4</sub> hemin structure on N-doped graphene featuring a FeN<sub>5</sub> axial coordination (Figure 4d).<sup>[73]</sup> The resulting FeN<sub>5</sub> SACs generate specific hydroxyl radicals and form Fe<sup>IV</sup> = O species, thereby achieving superior ORR properties and switching anodic/cathodic electrochemiluminescence



www.advmat.de

(ECL). It is also noted that the natural hemoglobin with apical His ligand bound to the central Fe ions is analogous to the heterogenous Fe-N<sub>E</sub> sites. Thereafter, Zhang et al. have produced a series of atomically dispersed Fe-N-C catalysts with different  $FeN_x$  (x = 4-6) structures by pyrolysis of sacrificial templates (Figure 4e).[74,75] The resulting medium-spin Fe<sup>III</sup>N<sub>5</sub> structure delivers higher turnover frequency and excellent reusability for the selective oxidation of C-H bond than that of the Fe<sup>III</sup>N<sub>6</sub> structure, and displays a similar O<sub>2</sub> transport property to the homogeneous hemoglobin. This innovative strategy can also be expanded for fabricating the other transition metal-based SACs with unique coordination geometry and micro-environment. Inspired by the square-pyramidal coordination mode in natural superoxide dismutase (SOD), Liao et al. have implanted a similar square-pyramidal Ni-N<sub>5</sub> site into carbon support to prepare nickel electrocatalyst in a controlled manner (Figure 4f).[76] Compared with the planar Ni-N<sub>4</sub> site, the Ni-N<sub>5</sub> catalytic site achieves better electrocatalytic performance for CO<sub>2</sub>-to-CO conversion in neutral aqueous solution.

#### 2.1.3. Bioinspired Modulation of Coordination Species for SACs

Notably, the nonmetal skeleton in natural enzymes is composed primarily of carbon (C), nitrogen (N), oxygen (O), sulfur (S), phosphorus (P), and chlorine (Cl) elements, which also play crucial roles in the stability and function of the whole enzyme framework. The specific composition and arrangement of those nonmetal elements in natural enzymes ensure the biochemical processes with high specificity and efficiency. As highlighted above, another critical aspect of engineering the microenvironments around the single-atom sites is introducing a secondary nonmetal heteroatom into the coordination sphere. Specifically, the heteroatom tethering strategy provides immense scope for adjusting the asymmetric charge distribution and coordination bond lengths, thus moderating the binding strength of intermediates and influencing electro-/photocatalytic reaction behaviors.

Apart from nitrogen as a coordinating atom from amino acids, sulfur is another essential element to form disulfide bonds (S-S) in the thiol group (-SH) of cysteine residues, which is crucial for stabilizing protein structures in metabolic reactions. [78] In the carbon supported metal SACs configuration, both N with an electronegativity of 3.04 and S of 2.58 are electron-withdrawing compared to C with the electronegativity of 2.55. Furthermore, S atom possesses less electronegativity and larger atomic radius compared to N atom, thus triggering higher electron localization within the metal center. Chen and coworkers have fabricated sulfurized Mn SACs (Mn<sub>SA</sub>/SNC) with MnN<sub>3</sub>S<sub>1</sub> moieties in the noncoplanar geometry (Figure 5a). [79] The local geometrical distortion in the Mn<sub>SA</sub>/SNC framework can improve the formation of additional S-O bonding and stabilize the \*COOH intermediates, thereby elevating the performance of electrochemical conversion of CO2 to CO. Similar asymmetric coordination strategy is also employed by Cui and coworkers for constructing Fe-S<sub>1</sub>N<sub>3</sub> geometric distortion with distinctive selfrelaxation behavior. [80] This Fe-S<sub>1</sub>N<sub>3</sub> SAC exhibits dynamic evolution of bond lengths, which renders optimized modulation of the adsorption energies and enhanced activity of electrochemical CO, RR.

As another representative nonmetal element, boron (B) atom is electron-donating with a much lower electronegativity (2.04) than that of C atoms, which can increase the electron density at the active site by electron-sharing effects. Typically, boron is involved in a variety of biological processes in cell division and sugar transportation, which can also influence enzyme activity indirectly. Zhao and colleagues have fabricated B, N cocoordinated SAC catalyst (Zn–B/N–C) to manipulate the s-band of Zn centers with intriguing electrocatalytic ORR activity. The ZnB<sub>2</sub>N<sub>2</sub> configuration is most stable with the distinctive  $3d^{10}4s^1$  character of Zn<sup>+</sup>, endowing with enough delocalized electrons and moderate adsorption ability with key oxygen intermediates (Figure 5b).

In biological systems, phosphorus element is often presence in the form of phosphate group (PO<sub>4</sub>3-), which is a key component of adenosine triphosphate (ATP), nucleotide, and phospholipid.[82] In the periodic table, phosphorus and nitrogen belong to the same main group with similar valence shell electron configuration. Furthermore, P heteroatom is also an effective electron donor with similar low electronegativity (2.19) and large atomic size compared to B atom, consequently creating additional charge accumulation and modulating the binding strength of reaction intermediates. For instance, Li et al. have imbedded single-atom Fe sites with less positive charge in the well-engineered FeN<sub>3</sub>P-centred single-atom catalyst (Figure 5c).<sup>[83]</sup> Comparable enzyme-like catalytic activity and kinetics are achieved with low barriers of surface O formation on the FeN<sub>3</sub>P SACs configuration. Benefitting from the intrinsic Fe-N<sub>3</sub>P active sites in another study, fast reaction kinetics and optimized adsorption/desorption energies of oxygen intermediates are favorable for boosting electrocatalytic ORR performance.[84] In addition, similar atomic Co<sub>1</sub>-P<sub>1</sub>N<sub>3</sub> interfacial structure is also observed in Wang's work by in situ phosphatizing. [85] Compared to the symmetric Co-N<sub>4</sub>, Co<sub>1</sub>-P<sub>1</sub>N<sub>3</sub> exhibits more favorable activity and durability for electrocatalytic HER.

Building upon heteroatom tethering, the in-plane coordination regulation can be further expanded to the out-of-plane coordination regulation in the first shell. The nonmetal elements of natural enzymes normally present in amino acid residues and functional groups, some of which act as axial ligands to the enzyme's metal centers. Generally, these ligands can be categorized into C-containing groups (-C, -COOH, etc.), Ncontaining groups  $(-N/-NH_2)$ , O-containing groups (-O, -OH, -OH)etc.), S-containing groups (-S/-SH), and halogen-containing ligands (-F/-Cl/-Br/-I etc.). These axial ligands can modulate the electronic properties of the central metals and adjust the substrate binding with indispensable biological roles. Inspired by the enzyme's configuration, Jiang and coworkers have fabricated a hemin—cysteine-Fe SACs (HCFe) framework involving Fmoc-l-cysteine, heme, and Fe<sup>2+</sup> coordination via supramolecular assembly approach (Figure 5d).[86] The as-constructed HCFe uniquely incorporates heme and [Fe-S] structures within its Fe−N<sub>4</sub> active centers, which significantly promote the intrinsic selectivity even beyond that of natural enzymes. In addition to the Fe-based natural enzymes, the vitamin B<sub>12</sub> enzyme is an organometallic compound including cobalt ions coordinated by

15214095, 0, Downloaded from https://adanceed.onlinelibrary.wiley.com/doi/10.1002/adma.202502131 by HONG KONG POL YTECHNIC UNIVERSITY HU NG HOM, Wiley Online Library on [28/09/2025]. See the Terms and Conditions (https://onlinelibrary.wiley.com/doi/10.1002/adma.202502131 by HONG KONG POL YTECHNIC UNIVERSITY HU NG HOM, Wiley Online Library on [28/09/2025]. See the Terms and Conditions (https://onlinelibrary.wiley.com/doi/10.1002/adma.202502131 by HONG KONG POL YTECHNIC UNIVERSITY HU NG HOM, Wiley Online Library on [28/09/2025]. See the Terms and Conditions (https://onlinelibrary.wiley.com/doi/10.1002/adma.202502131 by HONG KONG POL YTECHNIC UNIVERSITY HU NG HOM, Wiley Online Library on [28/09/2025]. See the Terms and Conditions (https://onlinelibrary.wiley.com/doi/10.1002/adma.202502131 by HONG KONG POL YTECHNIC UNIVERSITY HU NG HOM, Wiley Online Library on [28/09/2025]. See the Terms and Conditions (https://onlinelibrary.wiley.com/doi/10.1002/adma.202502131 by HONG KONG POL YTECHNIC UNIVERSITY HU NG HOM, Wiley Online Library on [28/09/2025]. See the Terms and Conditions (https://onlinelibrary.wiley.com/doi/10.1002/adma.202502131 by HONG KONG POL YTECHNIC UNIVERSITY HU NG HOM. Wiley Online Library on [28/09/2025]. See the Terms and Conditions (https://onlinelibrary.wiley.com/doi/10.1002/adma.202502131 by HONG KONG POL YTECHNIC UNIVERSITY HU NG HOM. Wiley Online Library on [28/09/2025]. See the Terms and Conditions (https://onlinelibrary.wiley.com/doi/10.1002/adma.202502131 by HONG KONG POL YTECHNIC UNIVERSITY HU NG HOM Wiley Online Library on [28/09/2025]. See the Terms and Conditions (https://onlinelibrary.wiley.com/doi/10.1002/adma.202502131 by HONG KONG POL YTECHNIC UNIVERSITY HU NG HOM Wiley Online Library on [28/09/2025]. See the Terms and Conditions (https://onlinelibrary.wiley.com/doi/10.1002/adma.202502131 by HONG KONG POL YTECHNIC UNIVERSITY HU NG HOM Wiley Online Library on [28/09/2025].

litions) on Wiley Online Library for rules of use; OA articles are governed by the applicable Creative Commons

#### **Bioinspired Regulation of Coordination Species**

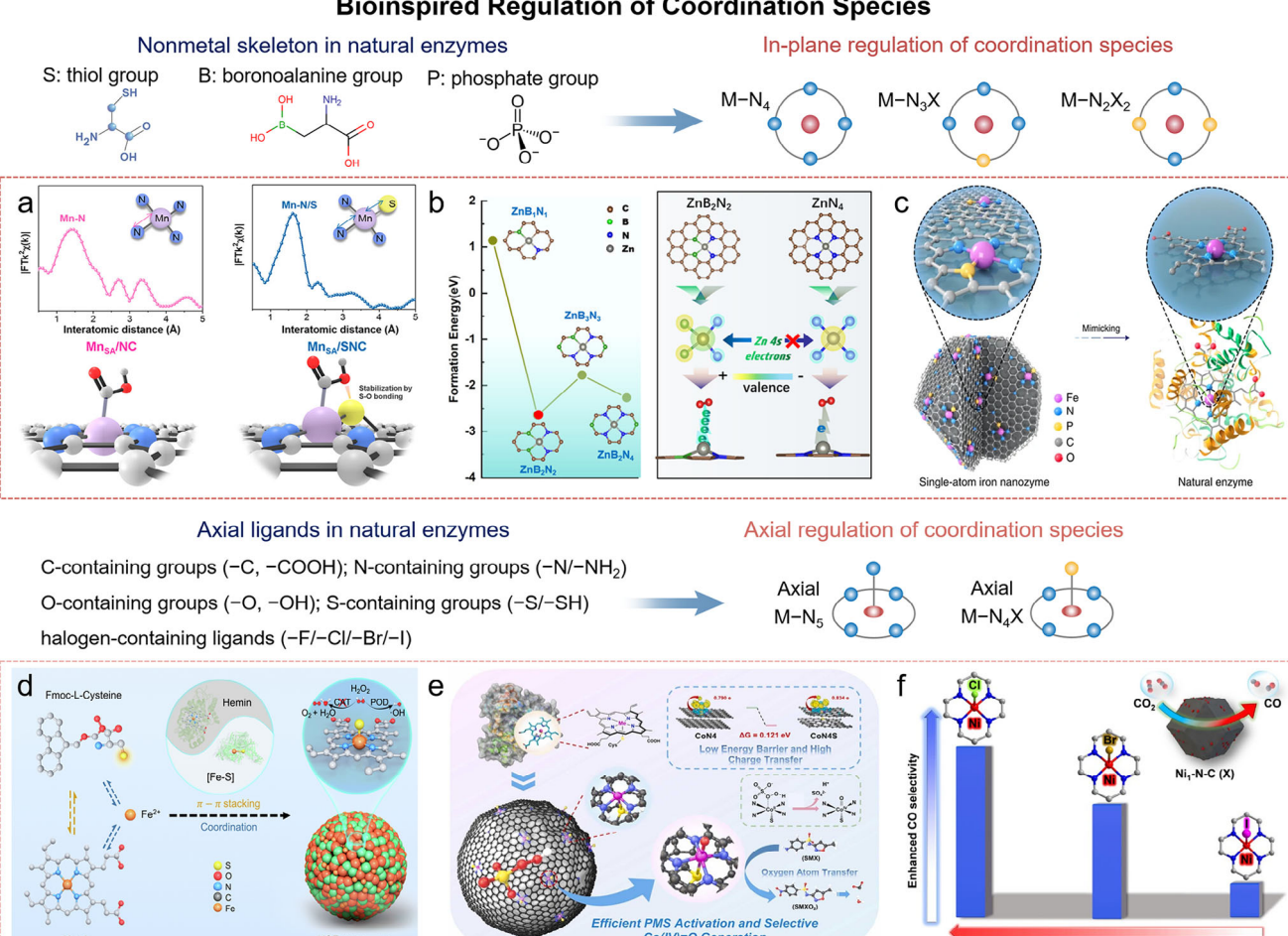


Figure 5. a) The EXAFS fitting curves in R space and the corresponding atomic structure models (inset), along with diagram of structure of MnSA/NC and MnSA/SNC. Adapted with permission. <sup>[79]</sup> Copyright 2021, American Chemical Society. b) Formation energy and diagram illustrating the enhanced charge transfer of ZnB<sub>2</sub>N<sub>2</sub> compared to the ZnN<sub>4</sub> moiety. Adapted with permission. <sup>[81]</sup> Copyright 2021, Wiley-VCH. c) The engineered FeN<sub>3</sub>P-centred single-atom nanozyme with excellent peroxidase-like activity. Adapted with permission. <sup>[83]</sup> Copyright 2021, Springer Nature. d) Illustration of the synthesis process for HCFe nanozyme. Adapted with permission. <sup>[86]</sup> Copyright 2024, Springer Nature. e) The bioinspired single-atom Co catalyst (CoN<sub>4</sub>S-CB) to activate peroxymonosulfate (PMS) for the effective degradation of sulfamethoxazole. Reproduced with permission. <sup>[87]</sup> Copyright 2024, Elsevier. f) Enhancing the efficiency and selectivity of CO<sub>2</sub> reduction by incorporating axially coordinated halogens into single-atom Ni catalysts. Reproduced with permission. <sup>[88]</sup> Copyright 2022, Springer Nature.

an axial ligand. In this case, Zhu's group have developed a bioinspired Co SACs with axial S coordination (CoN<sub>4</sub>S-CB) for peroxymonosulfate (PMS) oxidation (Figure 5e).<sup>[87]</sup> Compared to the CoN<sub>4</sub> counterparts, the axial S coordination is adopted to modulate the 3d orbital electron distribution of atomic Co centers for selective high-valent Co-oxo species (Co<sup>IV</sup> = O) generation. While halogen atoms with unique  $ns^2np^5$  electron configuration cannot directly coordinate to central metal sites in-plane, they are also suitable to serve as axial ligand bonded with metal centers individually out-of-plane. For instance, Jiang et al. decorate atomic Ni centers (Ni-N<sub>4</sub>) with different axial halogen atoms (Cl, Br, and I) by a post metal halide modification (PMHM) strategy (Figure 5f).<sup>[88]</sup> Particularly, the planar Ni-N<sub>4</sub> sites with the most electronegative chlorine atom can facilitate the formation of

\*COOH intermediate, resulting in a remarkable electrocatalytic CO<sub>2</sub> reduction performance.

## 2.2. Bioinspired Engineering of the Second/Long-Range Coordination of SACs

Besides engineering the first coordination shell, the second to long-range coordination sphere in SACs can also be precisely manipulated to tune the reactivity of the central atoms indirectly. Motivated by the natural residues and molecules in the second coordination sphere of metalloenzymes, multiple bioinspired strategies including heteroatoms doping, dual-metallic sites, nano-single-atom-sites, and metal-support interaction have





been developed to tune the longer-range electron delocalization to achieve the desirable activity, selectivity, and stability during electro-/photocatalysis of SACs.

## 2.2.1. Bioinspired Heteroatoms Doping within the SACs Configuration

In the case of pristine M-N<sub>4</sub> carbon-based SACs model, the second and long-range coordination are mainly composed of carbon atom matrix. Precise doping of nonmetal heteroatoms within second or long-range coordination spheres can weaken the strong electron-withdrawing ability of the proximal N atoms while preserving the primary M-N<sub>4</sub> skeleton.<sup>[89]</sup> Noticeably, this coordination environment modulation further induces electron delocalization and alleviates strong adsorption of intermediates at the SACs metal centers. In the biological metabolic process, the unique arrangement of proximal amino acid residues also plays specific roles for the noncovalent interactions in the second coordination spheres. As one typical example for enzymatic dehalogenation, the reductive dehalogenase (Rdh) mainly consists of a cobalt ionic center and a binding pocket with optimal noncovalent interactions, thereby activating the carbon-halogen bonds with optimized local electric field. Wu and coworkers have developed single-atomic Co sites supported on carbon doped boron nitride (BCN) (Co SAs/BCN) by a supramolecular controlled pyrolysis strategy to simulate the Rdh configuration (Figure 6a). [90] The as-fabricated Co SAs/BCN with locally polarized B-N bonds can reinforce the interaction between organochlorides and Co SAs/BCN by exerting electric fields onto C-Cl, thus boosting dehalogenation kinetics. Later, Zhang et al. synthesized a coordination polymer-based dual-site nickel SACs with Ni metal centers and 3,3'-diaminobenzidine ligands (Ni-DAB) to simulate the isolated substrate-binding pockets in coenzyme-independent oxidases (Figure 6b).[91] The Ni metal center and the C atom in the ligand play their respective roles as the specific uric acid (UA) and O2 binding sites, thereby realizing substrate specificity for the oxidation of UA in the biofuel cell.

In addition to the heteroatoms doping within the in-plane supports, the nonmetal coordination atom can also be located on the out-of-plane positions. Noticeably, the flexible and dynamic arrangement of amino acid residues in confined optimized enzyme space is crucial for achieving high catalytic activity and specificity. Inspired by the remarkable systems in nature, similar heterogenous 3D SACs configuration is primarily achieved by tuning spatial confinement with heteroatoms-containing functional groups modification. Hyeon and colleagues have successfully incorporated cooperative Brønsted acid-single atom Co catalytic sites within a precisely engineered metal-organic framework (MOF) (Figure 6c). [92] The dual-site cooperation by Co single-atom sites onto the Ti-oxo clusters and Brønsted acidic P-OH moieties ensures significant improvement in visible light photocatalytic hydrogen production. Inspired by natural hydrolytic enzymes, Lou and coworkers have developed a second coordination sphere engineering strategy to preorganize amino acids around metal ions and organic ligands of MOFs into a scaffold architecture containing dual catalytic active sites (Figure 6d).[93] The accessible Zn active metal sites in the first coordination shell display Lewis acidmediated pathway, where a new hydrogen bond interaction site is generated by a serine with a hydroxyl group side chain. The versatility of those dual accessible active sites promotes high-efficient hydrolysis of amide-containing pollutants for environmental remediation.

#### 2.2.2. Bioinspired Collaboration of Dual-Metallic Sites for SACs

In natural enzymes, metal sites are not only present in the active sites but also in cofactors which are integral to the enzyme's biological function. In conventional SACs, usually only one kind of active center is included and therefore it is challenging for these SACs to achieve multielectron/proton transfer in heterogenous electro-/photocatalysis. To address this limitation, incorporating a second metal to form dual diatomic site configurations (DACs) can combine the advantages of both metals with correlated atomic structures, unique local coordination, and tunable chemical states. [94,95] This dual-metallic sites collaboration engineering strategy can optimize the adsorbed energies for complex reactants/intermediates, modulate multiple reaction pathways, and enhance electro-/photocatalytic efficiencies. [34,96,97]

The configuration of homometallic and heterometallic diatomic pairs can be classified into three subcategories based on their metal-bonding properties: metal-metal bonded adjacent diatoms, coordinated atom-bridged bimetal sites, and cofacially separated bimetal sites (Figure 7). Specifically, Bu et al. have constructed dual Fe sites with Fe-Fe bonding anchored on S, N-codoped carbon matrix (Fe<sub>2</sub>N<sub>6</sub>-S) via a host-guest encapsulation strategy to mimic the natural ferredoxin (Figure 7a).[98] Compared to the conventional Fe SACs, the neighboring Fe sites can achieve the optimized adsorption of oxygen molecules, facilitate the O-O bond breaking, and balance the OH\* intermediate over adsorption behavior. The installation of S heteroatoms can further elaborate the whole electronic structure and decrease the reaction barriers for OOH\* formation. In this regard, the as-prepared Fe<sub>2</sub>N<sub>6</sub>-S homogeneous configurations with additional Fe and S sites as "dual modulators" can achieve enhanced electrocatalytic ORR activity and encouraging Zn-air batteries performance. Inspired by the structural and functional models of natural CcO, a series of homonuclear diatomic iron sites with different atomic configurations were also constructed by Zhang and coworkers.[99] As illustrated in Figure 7b, those as-obtained Fe DACs are designated as saturated and unsaturated separated dual single-atom Fe sites, direct metal-metal bonding and N-bridged dual-atom Fe sites, respectively. Among them, the Fe DACs with direct Fe-Fe bonding configuration exhibits the optimized balance between the adsorption and desorption pathway, thus facilitating the remarkable oxidase-like activity and excellent antifouling osmotic energy

Besides the bioinspired homometallic diatomic pairs, the hetero-paired bimetallic coordination along with two different central metal sites displays different electronic structures, leading to the structural deformation and charge polarization near the Fermi level. More importantly, DACs with hetero-paired bimetallic sites can effectively modulate the electronic states change and tune the absorption/desorption formations with

15214095, 0, Downloaded from https://advanced.onlinelibrary.wiley.com/doi/10.1002/adma.202502131 by HONG KONG POLYTECHNIC UNIVERSITY HU NG HOM, Wiley Online Library on [28/09/2025]. See the Terms

and-conditions) on Wiley Online Library for rules of use; OA articles are governed by the applicable Creative Commons

### **Bioinspired Heteroatoms Doping within the SACs Configuration**

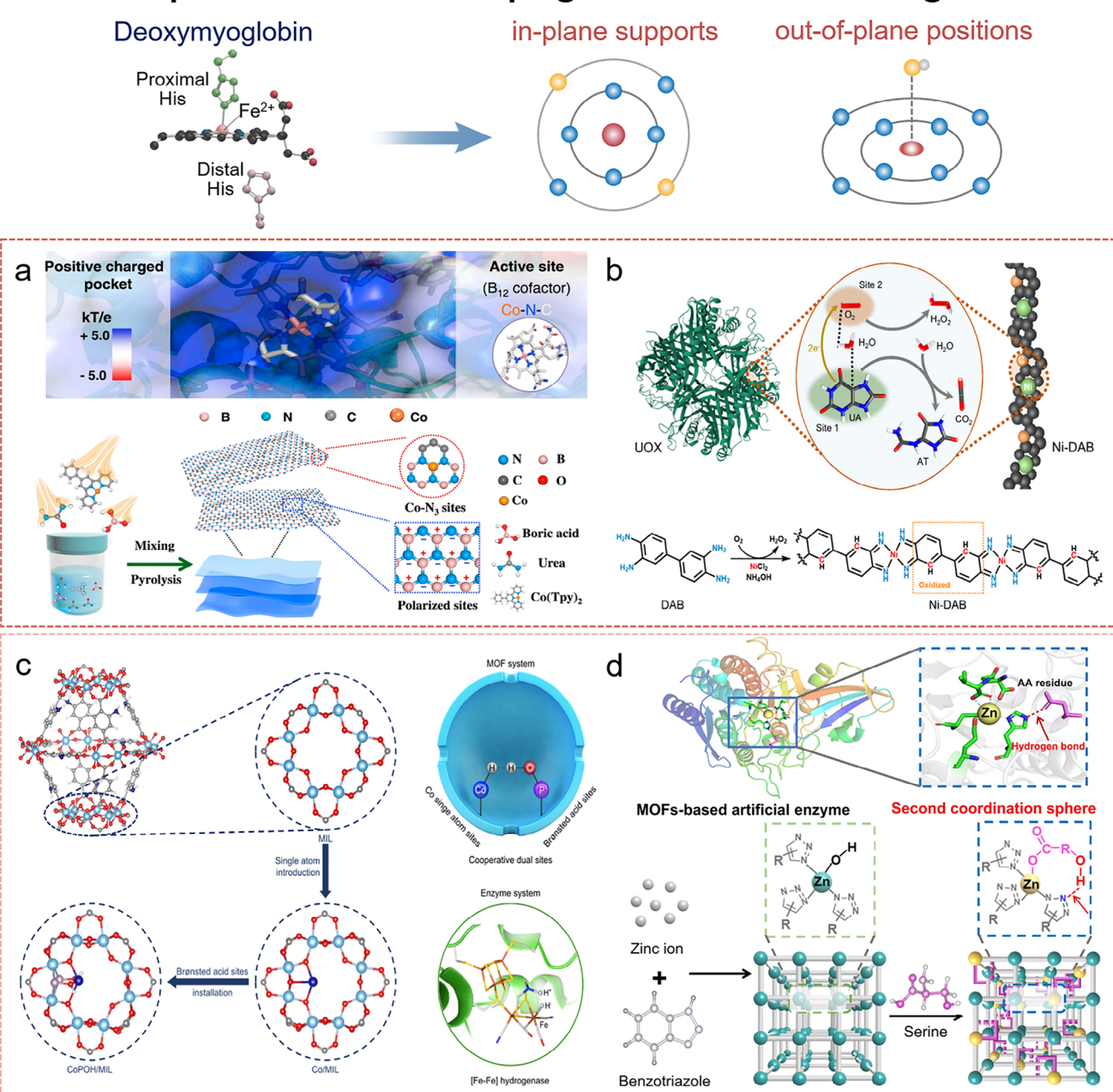


Figure 6. a) Surface static electricity depiction of the Rdh, with the potential contour ranging from +5.0 (blue) to -5.0 (red) k<sub>B</sub>Te<sup>-1</sup>. Diagram illustrating the preparation of the single-atom catalyst featuring atomically dispersed Co sites and polarized supports. Adapted under the terms of the CC-BY Creative Commons Attribution 4.0 International License.<sup>[90]</sup> Copyright 2021, The Author(s), Springer Nature. b) Diagram of catalysis of UA oxidation utilizing the independent dual sites of the natural UOX and Ni-DAB. Synthesis outline of Ni-DAB. Reproduced under the terms of the CC-BY Creative Commons Attribution 4.0 International License.<sup>[91]</sup> Copyright 2024, The Author(s), Springer Nature. c) Diagram of the synthesis approach for the cooperative Brønsted acid-single atom catalyst, referred to as CoPOH/MIL. Crucial intermediates of cooperative dual sites in both MOF and enzymatic systems. The nearby metal active site and Brønsted acid site collaborate synergistically by positioning the proton and hydride in close proximity. Reproduced with permission.<sup>[92]</sup> Copyright 2025, American Chemical Society. d) Diagram showing the natural hydrolytic enzyme carboxypeptidase (CPA) and its active site midazole group in a metal complex creates a secondary coordination sphere with a nearby amino acid residue. The dual catalytic active site groups in ZAF(Ser) are situated in the primary and secondary coordination spheres, resembling the Lewis acidic active site and the common oxygen anion active site found in hydrolase. Reproduced under the terms of the CC-BY Creative Commons Attribution 4.0 International License.<sup>[93]</sup> Copyright 2023, The Author(s), Springer Nature.

15214059. D. Downloaded from thtps://advance.onlinelibrary.wiley.com/oi/01/01/02/adna.2025/231 by HONG KONG POLYTECHNIC UNIVERSTY HU NG HOM, Wiley Online Library on (128/09/2025). See the Terms and Conditions (https://onlinelibrary.wiley.com/emrs-and-conditions) on Wiley Online Library for rules of use; OA articles as a governed by the applicable Creative Commons

#### **Bioinspired Collaboration of Dual-metallic Sites**

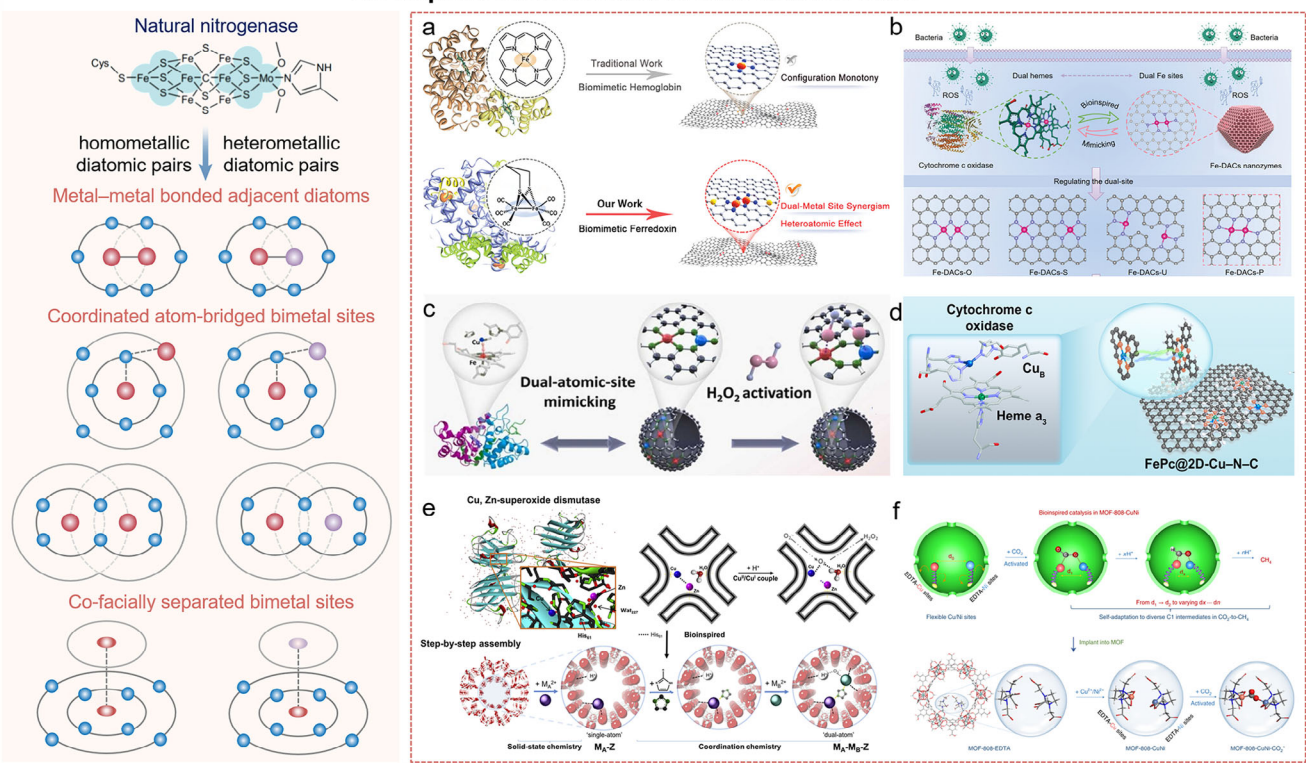


Figure 7. a) A dual metal Fe-based ORR catalyst (Fe<sub>2</sub>N<sub>6</sub>-S) featuring Fe-Fe dual sites and S sites to mimic the catalytic center of ferredoxin. Reproduced with permission.<sup>[98]</sup> Copyright 2024, Wiley-VCH. b) Diagram of effective osmotic energy transformation using bioinspired antifouling homonuclear diatomic iron composite membranes. Adapted with permission. [99] Copyright 2024, Wiley-VCH. c) Schematic diagram of developing atomically dispersed Fe-Cu catalysts on nitrogen-doped carbon nanospheres, which enhance H2O2 activation and therapeutic efficiency in the tumor microenvironment. Adapted with permission. [100] Copyright 2023, Elsevier. d) Structure of FePc@2D-Cu–N–C SAzymes and cytochrome c oxidase. Adapted under the terms of the CC-BY Creative Commons Attribution 4.0 International License. [33] Copyright 2024, The Author(s), Springer Nature. e) Diagram of the bioinspired "step-by-step" assembly method. Photo of the enzyme structure and active site of the natural Cu, Zn-SOD enzyme. Reproduced with permission.[101] Copyright 2022, Elsevier. f) The adaptable DMSPs for self-regulating  $CO_2$ -to- $CH_4$  photoreduction. Diagram illustrating bioinspired  $CO_2$  photoreduction in MOF-808-CuNi. Reproduced with permission. [102] Copyright 2021, Springer Nature.

different intermediates, achieving the synergistic effects for enhancement of a variety of electro-/photo-catalytic reactions.[96] Based on the natural CcO configuration composed of two hemes (heme a and a<sub>3</sub>) and copper centers (Cu<sub>A</sub> and Cu<sub>B</sub>), Liu and coworkercoworkers fabricate Fe-Cu hetero-binuclear active sites anchored into hollow nitrogen-doped carbon framework (Fe-CuNC) by a template-assistant strategy (Figure 7c). [100] The asprepared FeCuNC catalyst with FeN<sub>4</sub>-CuN<sub>3</sub> active sites displays lower dissociative adsorption energy and faster H2O2 reduction ability than those of single Fe sites. This bioinspired dual-metallic sites collaboration can be combined with spatial engineering strategy to further take the 3D spatial arrangement into consideration. Attractively, Wong's group develop a spatial engineering strategy to incorporate Fe-N<sub>4</sub> and Cu-N<sub>4</sub> dual-atomic sites with vertically stacked geometry (FePc@2D-Cu-N-C) to mimic the spatial configuration in natural CcO (Figure 7d).[33] Compared to planar Fe–Cu dual-atomic pair in 2D framework (2D-FeCu-N-C), this FePc@2D-Cu-N-C structure featuring 3D spatial Fe-Cu binuclear sites possesses stronger electronic coupling and stronger O2 activation capacity, accompanied by CcO-like electron transfer process and reaction pathway.

Apart from dual-metallic sites anchored on carbon-based supports, decorating the diatomic pairs into the regular pores of the supports is also an effective strategy to develop bioinspired DACs with impressive properties. For example, Lo et al. report a bioinspired "step-by-step" approach to assemble two late 3d metal cations (M<sup>2+</sup>) as "dual atoms" within ZSM-5 zeolitic microporous scaffolds (Figure 7e). [101] The neighboring  $M_1-M_2$ supported dual atoms display unique synergistic advantage and tertiary structure around the zeolitic supports. Noticeably, the metal active sites and the bridging histidine (His<sub>61</sub>) in native Cu, Zn-SOD enzyme are precisely engineered and simulated into the Zn<sub>A</sub>-Cu<sub>B</sub>-Z solid atomic catalysts. In another work, Zhong's group incorporated flexible Cu and Ni dual-metal-site pairs (DM-SPs) into a MOF-808 porous matrix via a facile capture process (MOF-808-CuNi) (Figure 7f).[102] To be specific, two flexible ethylenediaminetetraacetic acid (EDTA) molecules are grafted onto rigid Zr-oxo clusters, further chelating Cu<sup>2+</sup> and Ni<sup>2+</sup> ions by dangling EDTA ligands to yield self-adaptive heteropaired bimetallic Cu-Ni sites. The resulting MOF-808-CuNi with flexible microenvironment can serve as bioinspired photocatalyst to fit mutative C<sub>1</sub> intermediates and achieve efficient CO<sub>2</sub>-to-CH<sub>4</sub> conversion.

15214095, 0, Downloaded from https://advanced.onlinelibrary.wiley.com/doi/10.1002/adma.202502131 by HONG KONG POLYTECHNIC UNIVERSITY HUNG HOM, Wiley Online Library on [28.09/2025]. See the Terms and Conditions (https://onlinelibrary.wiley.

com/terms-and-conditions) on Wiley Online Library for rules of use; OA articles are governed by the applicable Creative Commons

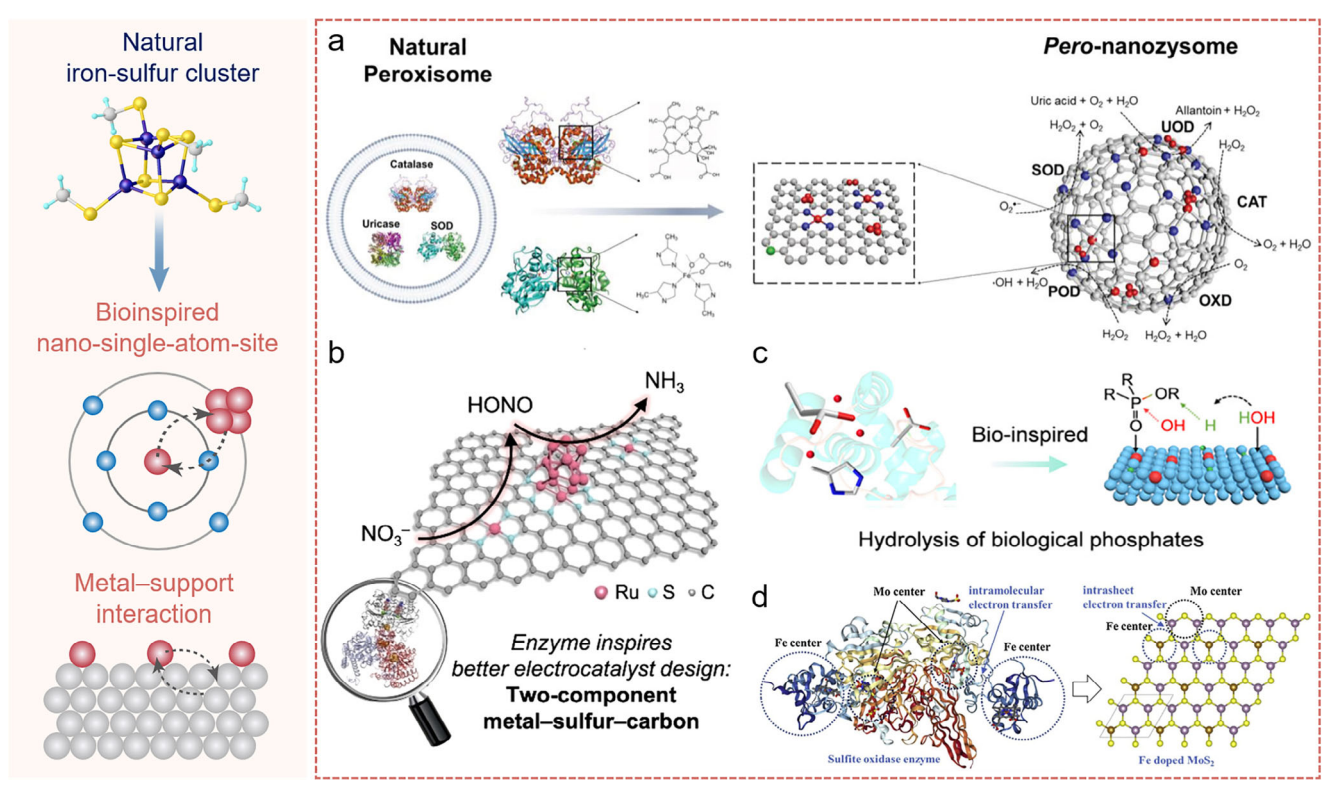


Figure 8. a) Diagram illustrating the design of an artificial peroxisome utilizing iron doping to a nanozyme (pero-nanozysome) to treat hyperuricemia and ischemic stroke. Adapted with permission. [108] Copyright 2020, Wiley-VCH. b) A metal–sulfur–carbon (M–S–C) catalyst to mimic enzyme function for electrochemical nitrate reduction. Adapted with permission. [109] Copyright 2024, Wiley-VCH. c) The Pt hydrides doping with single atom Ce exhibit the enhanced phosphatase-like activity for phosphate hydrolysis. Adapted with permission.[114] Copyright 2024, American Chemical Society. d) The single Fe atoms in MoS<sub>2</sub> nanosheets as effective catalysts for sulfite activation inspired by sulfite oxidase. Reproduced with permission. [116] Copyright 2020, Elsevier.

#### 2.2.3. Bioinspired Nanosingle-Atom-Site Catalysts

Compared with nano catalysts, SACs and DACs indeed possess maximal exposed active sites and higher metal utilization. However, due to the limitation of metal loading, these atomic metal sites are unable to satisfy the requirements of large atomic ensembles to completely replace nano catalysts. Besides the metal centers in enzymes and proteins, the cofactor consisting of a group of atoms or molecules also plays crucial roles in complex biochemical transformations.[103] As one of the most classic cofactor clusters, the iron-sulfur cluster is composed of iron and sulfur atoms with specific geometric configurations and acts as key components in electron transport chains.[104] In this regard, a family of nanosingle-atom-site catalysts (NSASCs) containing both single-atom sites and cluster/nanoparticle sites are developed to make up for the respective limitations of SACs and nanoparticles.[105,106] Furthermore, the electronic interaction between electron-rich nanoparticles with zero valence state and electron-deficient SACs with partial positive charges in NSASCs can synergistically catalyze diverse complex reactions.[107] As illustrated in Figure 8a, Gao and coworkercoworkers incorporate iron and nitrogen elements into hollow carbon matrix to give Fe-N<sub>4</sub> coordination together with atomic Fe cluster to form an artificial peroxisome. [108] The Fe clusters as reversible cofactors and the Fe-N<sub>4</sub> sites as prosthetic group can work together elaborately to exhibit stable peroxisomal-like activities. Another typical paradigm for a two-component enzyme-mimicking metal-sulfur-carbon (M-S-C) catalyst is inspired by the structural enzymology of the nitrogenase and the nitrate reductase (Figure 8b). [109] Specially, Wang et al. have fabricated coexisting ruthenium single atoms (Ru SAs) and nanoparticles (Ru NPs) supported on S-C frameworks ((SAs+NPs)/S-C) with unique synergistic interactions. The S-coordinated Ru SAs can promote the formation of nitrous acid (HONO) intermediates and subsequent nitrate reduction reaction (NitRR) on the adjacent Ru NPs, achieving exceptional ammonia yield rates. To mimic two typical antioxidase of human mitochondrial manganese SOD and erythrocyte catalase, Shi and coworkercoworkers assemble active Mn<sup>III</sup> sites in porphyrin skeletons interconnected by the Zn<sub>2</sub>(COO)<sub>4</sub> paddlewheel metal nodes to give a 2D nanosheet MOF. [110] The Zn<sup>2+</sup> in Zn<sub>2</sub>(COO)<sub>4</sub> clusters can upregulate the redox potential of MnIII centers in coordinated manganese porphyrin ligands, promoting the SOD- and catalase-like activities.

#### 2.2.4. Bioinspired Design of Metal-Support Interaction for SACs

Besides the metal-metal interaction in the second/longer-range coordination, the interaction between metal ions/clusters and the protein matrix in natural enzymes is also a key consideration



www.advmat.de

in biological processes. In the SACs-based heterogenous catalysis, while the single-atomic centers serve as the active sites for substrate binding and activation, their unique interaction with the supports is also essential for stabilizing the single atom active site with the reaction intermediate.[111-113] Inspired by the natural phosphatase enzyme, Zhu and coworkercoworkers have doped single-atom Ce sites onto Pt hydrides support (Ce/Pt-H) (Figure 8c).[114] To mimic the biological phosphate hydrolysis adequately, the atomically dispersed Ce centers can serve as Lewis acid sites to coordinate with phosphate groups, whereas the surface hydrides on Pt supports can accelerate the cleavage of H<sub>2</sub>O molecules and nucleophilic attack on phosphoric ester bonds. In the natural sulfite oxidase, the atomic Fe and Mo sites are coordinated with biomacromolecules to promote the synergistic sulfite oxidation catalysis. [115] Alternatively, Liu and colleagues confine single Fe atoms into two-dimensional MoS<sub>2</sub> nanosheets (Fe<sub>x</sub>Mo<sub>1-x</sub>S<sub>2</sub>) via a one-pot hydrothermal method (Figure 8d).<sup>[116]</sup> The as-synthesized Fe<sub>x</sub>Mo<sub>1-x</sub>S<sub>2</sub> catalyst can achieve efficient degradation of organic pollutants through a synergistic Mo-Fe catalysis mechanism.

## 2.3. Bioinspired Guidelines for Engineering Outer Microenvironment of SACs

Beyond the active sites and the first/second coordination spheres, the outer microenvironment in enzymes consist of amino acids and peptides from the protein matrix near the catalytic pocket, which can serve as the biological channels for substrate/product transport and proton/electron transport. This section focuses on engineering bioinspired outer microenvironment of SACs with unique noncovalent interactions and oriented mass/proton/electron transfer, collectively influencing the structural integrity and catalytic properties.

#### 2.3.1. Bioinspired Design of Noncovalent Interactions in SACs

The noncovalent interactions ensure the tertiary structure of natural enzymes in the dynamic conformational transformation and specific substrate binding.<sup>[117]</sup> Fundamentally, besides the covalent interactions among the metal—coordination species, metal—metal, and metal—support, the noncovalent interactions can also modify the microenvironment and offer vast opportunities to achieve more complex functionalities in SACs-based heterogenous catalysis process.<sup>[118]</sup> In this way, various bioinspired noncovalent interactions including hydrophobic interactions, van der Waals forces, and hydrogen bonding are further employed for designing effective SACs from the perspective of both the micro/nano scales and atomic/molecular scales.

Different from the homogeneous catalysis where the catalysts and reactants are in a common physical phase, typical solid-state catalysts are in separate physical phases with the reactants (e.g., gas or liquid) in heterogeneous catalysis. [119] In this context, hydrophobic interactions are beneficial for gathering non-polar or hydrophobic reactants to create concentrated microenvironments around the catalyst surface and potentially accelerate the catalytic process. [120] Taking nature as inspiration on the micro/nano scales, there are countless waxy mastoids on the sur-

face of the lotus leaf, thereby forming a multilevel hydrophobic layer with impressive gas-trapping phenomenon. Chen and coworkercoworkers have constructed an analogous multiscale hydrophobic surface of the single-atom Fe-N<sub>4</sub> catalyst (Fe-FNC) similar with the "lotus effect" via a facile gas-phase fluorinationmodulation strategy (Figure 9a).[121] The as-developed hydrophobic Fe-FNC catalyst can accelerate the diffusion and adsorption of oxygen reactants with the formation of triple-phase interfaces, facilitating the O2-related reactions kinetics and boosting the electrocatalytic ORR performance. In general, hydrophobic interaction is one of the critical factors in protein folding, where the nonpolar amino acids can create a hydrophobic region away from the aqueous environment in the interior of enzymes. Intriguingly, Zhang's group have developed a bioinspired atomically isolated Cu<sup>+</sup> species in ZnSe colloidal quantum wells (Cu/ZnSe), containing spatially organized NH<sub>2</sub>···Cu–Se(–Zn) moieties as distinctive synergistic catalytic pockets. Moreover, the resultant Cu/ZnSe with vicinal octylamine (OA) and oleyl amine (OLA) ligand layer can form the hydrophobic outer spheres and achieve an enriched local CO2 concentration, thus promoting CO<sub>2</sub>-to-ethanol photoconversion (Figure 9b).<sup>[122]</sup> Drawing inspiration from natural methane monooxygenases (MMOs), Jiang and coworkers have incorporated Fe-porphyrin into MOF (UiO-66) with hydrophobic modification of long-chain fatty acids (Fe<sup>3+</sup>@UiO-66-C<sub>n</sub>) (Figure 9c).<sup>[123]</sup> Importantly, this hydrophobic modification strategy can effectively modulate the electronic state of single-atomic Fe active sites in Fe<sup>3+</sup>@UiO-66-C<sub>n</sub> framework and tune the selectivity towards CH<sub>3</sub>OH in CH<sub>4</sub> oxidation.

Van der Waals force arises from temporary dipoles when electrons are unevenly distributed within molecules. Such shortrange forces can promote the close packing of amino acid side chains to maintain the overall stability of natural enzymes. To take full advantage of both hydrophobic interaction and van der Waals attraction, Qiao et al. have constructed a zinc-doped carbon nitride/silica framework with the silylation of trimethylchlorosilane (TMCS) as hydrophobic singleatom photocatalyst (Zn/CN@Si) (Figure 9d).[124] This hydrophobic interface microenvironment of Zn/CN@Si with an unique O2 (gas)-H2O2 (liquid)-catalyst (solid) three-phase interface can display strong van der Waals attraction towards hydrophobic O<sub>2</sub> molecules from aqueous systems. At the same time, the weak electrostatic attraction to H2O2 molecules is beneficial to release hydrophilic H2O2 products away from the Zn/CN@Si interface. Such a "capture-release" catalysis strategy can promote the both the mass-transfer and reaction kinetics processes, thus achieving a satisfactory H<sub>2</sub>O<sub>2</sub> generation

Hydrogen bonding is one of the critical noncovalent interactions in the atomic/molecular scale, where a hydrogen atom is covalently bonded to an electronegative atom (O or N) and accompanied by hydrogen bond formation with another electronegative atom. Such a weak noncovalent interaction is typically involved in maintaining the secondary structure of proteins (e.g., alpha-helix and beta-sheet) and inducing the conformational change in natural enzymes. [125] In the case of heterogenous catalytic reaction kinetics, the interfacial hydrogen-bond networks play an integral role in accelerating the proton transfer and stabilize the transition states. [126,127] Recent work has confirmed that the connectivity of

www.advmat.de

15214095, 0, Downloaded from https://advanced.onlinelibrary.wiley.com/doi/10.1002/adma.202502131 by HONG KONG POLYTECHNIC UNIVERSITY HU NG HOM, Wiley Online Library on [28:09:2025]. See the Terms

conditions) on Wiley Online Library for rules of use; OA articles are governed by the applicable Creative Common

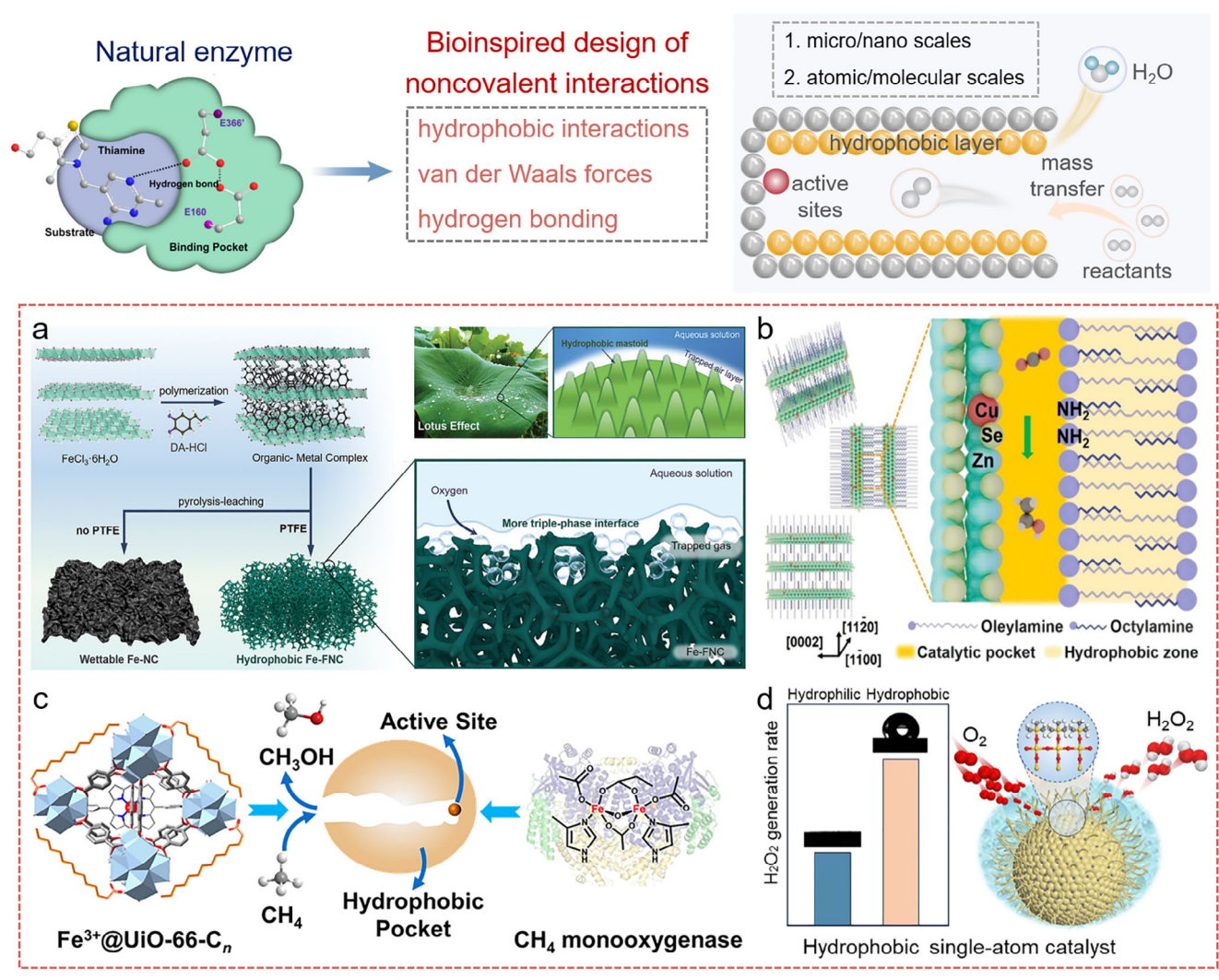


**Figure 9.** a) Diagram of the synthesizing approach for wettable Fe-NC and hydrophobic Fe-FNC. The inspiration from lotus: employing a hydrophobic surface to capture a layer of gas at the solution–solid interface. Illustration of the "lotus effect" on the Fe-FNC surface for reducing aqueous O<sub>2</sub>. Reproduced with permission.<sup>[121]</sup> Copyright 2023, Wiley-VCH. b) Diagram illustrating the loosely assembled Cu/ZnSe QWs, along with the nearby ligand layer made of OA and OLA, creates a catalytic pocket. Reproduced with permission.<sup>[122]</sup> Copyright 2024, the American Association for the Advancement of Science. c) Embedding Fe-porphyrin in a metal–organic framework with fatty acids enables selective CH<sub>4</sub> to CH<sub>3</sub>OH conversion, with hydrophobic fatty acids enhancing selectivity by modifying Fe site electronics, boosting CH<sub>4</sub> adsorption, and controlling H<sub>2</sub>O<sub>2</sub> concentration. Reproduced with permission.<sup>[123]</sup> Copyright 2023, Elsevier. d) Schematic diagram of hydrophobic single-atom photocatalyst (Zn/CN@Si). Reproduced under the terms of the CC-BY Creative Commons Attribution 3.0 Unported License.<sup>[124]</sup> Copyright 2024, The Author(s), Chinese Chemical Society. This figure has been published in CCS Chemistry 2024; Hydrophobic Zn Single-Atom Catalyst for Efficient Photosynthesis of Hydrogen Peroxide is available online at https://doi.org/10.31635/ccschem.024.202404694.

hydrogen-bond networks in the electric double layer (EDL) plays a dominant role in regulating the electrocatalytic activities.  $^{[128]}$  Based on theoretical calculation, Liu et al. demonstrated that hydrogen bonding is vital for generating polar intermediates on single nickel atom catalysts, which would result in high CO $_2$ RR selectivity.  $^{[129]}$  Additionally, Yin's group have fabricated atomically dispersed lanthanide metal material with a La-N $_4$  configuration (La-N-C), which can serve as "electrons bridge" to promote the electrons transfer from the N-C support to the perdisulfate (PDS) molecule.  $^{[130]}$  The formation of hydrogen-bond on the surface of La-N-C catalyst can efficiently promote the adsorption and activation of PDS substrates.

#### 2.3.2. Bioinspired Design of Mass/Proton/Electron Transfer in SACs

In heterogenous catalysis, efficient mass transfer is essential for the diffusion and movement of molecules, thus promoting the adsorption of reactants and the subsequent desorption of products. [131] It is worth noting that plenty of supports in the above bioinspired heterogenous SACs are typical 3D nanoconfined frameworks to adequately expose active sites and improve overall catalytic activity. With regards to the bioinspired approach, numerous porous biological systems with optimal mass transfer characteristic have been witnessed in both plants and animals across all scales. Among them, ordered porous structures





www.advmat.de

are one of typical products of natural evolution with high degree of organization on the microscopic or nanoscopic levels.  $^{[132]}$  As illustrated in **Figure 10**a, the sieve tubes in plants can deliver substances over confined frameworks in a controlled and precise manner. Inspired by the delicate well-confined channel structure in sieve tubes, Zhang et al. confine abundant Fe single-atom sites into the mesopores of ordered mesoporous silica (SBA-15) templates (channel-Fe\_{SAC}).  $^{[133]}$  The well-confined and long-range ordered channel-Fe\_SAC structure can create individual and stable catalytic sites with unique localized capture-catalysis microenvironments, and thus significantly inhibit the migration of polysul-fide for efficient lithium–sulfur batteries.

It is worth noting that the transportation of molecular reactants, products, ions and electrons in heterogenous catalysis needs to pass through different phases in the reaction medium.[134] Hence, hierarchically porous structures with optimized networks have been extensively investigated to reduce diffusion and transport limitations in nonhierarchical structures.[135] In terms of the multiscale characteristics in hierarchically porous structures, micropores (with diameters less than 2 nm) are crucial for exposing massive active sites for molecular adsorption; Moreover, mesopores (with diameters between 2 and 50 nm) can promote the diffusion and accessibility from catalysts to reactants;[136] Meanwhile, macropores (with diameters greater than 50 nm) can allow larger molecules or ions channels for fluid flow, thus enhancing mass transfer and reduce diffusion limitations. The hierarchical transport networks in natural systems can provide innovative inspiration for the design of optimal SAC architectures. Li and coworkers have recently decorated isolated asymmetric coordinated V-S<sub>1</sub>N<sub>3</sub> sites onto interconnected porous structures as inspired by the natural alveoli tissue (Figure 10b). [137] The well-distributed enzyme-mimic V-S<sub>1</sub>N<sub>3</sub> catalytic centers on the wall of alveoli-inspired interconnected porous carbon matrix can trigger fast diffusion and enhanced sulfur adsorption-catalytic conversion. Wang and coworkers also capitalize on the unique organic texture and function of jellyfish to design advanced ORR electrocatalysts (Figure 10c).[138] Specifically, the jellyfish-inspired Fe clusters and atomic Cu+ sites connected by carbon nanotubes (CNTs) in the whole hierarchical porous structures can ensure rapid mass transport and enhance the electron redistribution between the Fe and Cu sites. Another fascinating strategy is inspired by the morphology and structure of sea anemones and seabed rocks (Figure 10d).[139] Subsequently, Qing and coworkers have designed and fabricated a self-supporting sea anemone-like structure with the coexistence of single-atom Co-N<sub>4</sub> sites and Co nanoparticles (NPs) in N-doped CNTs, whereas activated microporous carbon fibers (ACF) derived from natural wood fibers serve as the seabed rock (Co/CoN<sub>4</sub>PCF). Advantageously, the ACF seabed rock with high conductivity and sufficient pores channels can promote the transport of electrons and electrolytes, whereas the atomic Co sites in sea anemones frameworks can anchor O2 and reaction intermediates. The synergistic effects of both seabed rock and sea anemones structures deliver impressive ORR performance.

Besides the mass transfer of various reactants/intermediates/products, the proton and electron transfer are also fundamental processes in the microenvironment of both the reaction interface and catalyst surface in heterogeneous catalysis. [140] Moreover, the proton coupled electron transfer

(PCET) is a representative mechanism for energy conversion in chemistry and biology. With regards to the biological ORR process by cytochrome c oxidases (CcOs), the external protons are transported to the heme-Cu sites via a specialized proton channel with the assistance of amino acid residues (Figure 11a). Beyond the channel-based transfer, the tyrosine phenolic hydroxyl groups are further employed to guide proton transfer within the local environment around the heme-Cu sites. Inspired by the unique proton channels and local proton relays in natural CcOs, Cao et al. have developed a Co-corrole-based porous organic polymer (POPs) by tuning the pore sizes and functionalizing active Co corrole molecular units. Notably, enhanced proton transfer is achieved both near the local active sites and within the channels, thereby delivering extraordinary electrocatalytic ORR and OER performances.

Flavin adenine dinucleotide (FAD) is a versatile redox-active cofactor in biological electron transfer. Motivated by FAD, Zhu and coworkers have incorporated single-atom Fe(III) sites into the AuFe/polydopamine (PDA) superparticles (AuFe/PDA) with branched nanostructures (Figure 11b).[143] Similar to the cofactor FAD, the optimized Fe(III)-coordinated AuFe/PDA with abundant phenolic hydroxyl and amino groups can promote H atom and electron transfer (ET) adequately, undergoing an artificialcofactor-mediated hydrogen atom transfer process to achieve enhanced glucose oxidase (GOX) reaction. Subsequently, this group have further embedded multiple nanocofactors (NCFs) including single atomic Fe sites, linkers, and zirconia nodes into crystalline UiO-67 MOF as the catalytic pocket (UiO-67-Fe) (Figure 11c).[144] Benefiting from the synergistic effect of three nanocofactors, enhanced ET efficiency of intermediates is induced by bare linkers and zirconia nodes, thus resulting in significant H<sub>2</sub>O<sub>2</sub> substrate activation on the linker-coupled atomic iron sites.

## 3. Bioinspired Heterogenous SACs for Electrocatalysis and Photocatalysis

Natural enzymes exhibit high catalytic activity at their active sites, many of which are metal-based.<sup>[145,146]</sup> However, replicating the complex structure of natural enzymes is challenging. In this section, we will review the progress in mimicking four major classes of enzymes, namely hydrogenase, nitrogenase, oxidase, and dehydrogenase by SACs (Table 2).

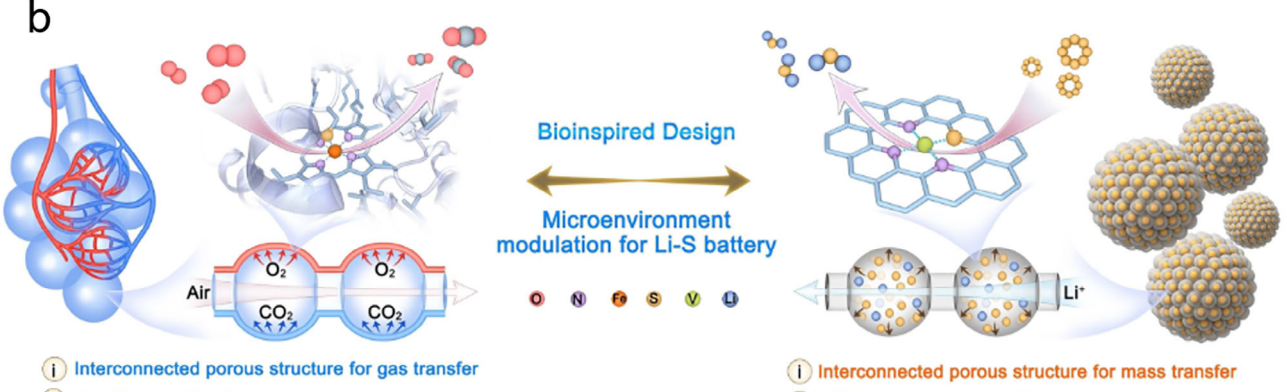
#### 3.1. Hydrogenase-Inspired Heterogenous SACs for H<sub>2</sub> Evolution

Hydrogen is considered a promising alternative energy source to address environmental concerns. Currently, noble metal catalysts such as platinum group metals remain state-of-the-art catalysts, whether as primary or cocatalysts. However, due to their high cost and limited availability on earth, the search for alternative catalysts is necessary. Hydrogenases, metalloenzyme that efficiently convert H<sup>+</sup>/H<sub>2</sub>, typically utilize iron and/or nickel at their active sites with an inner coordination sphere to achieve low overpotentials and high turnover rates.<sup>[147,148]</sup> The archetypal *Desulfovibrio gigas* NiFe hydrogenase is a globular heterodimer containing an NiFe dinuclear center, three nonprotein ligands (one CO and two CN– ligands) attached to the iron atom, and

15214095, 0, Downloaded from https://advanced.onlinelibrary.wiley.com/doi/10.1002/adma.202502131 by HONG KONG POLYTECHNIC UNIVERSITY HU NG HOM, Wiley Online Library on [28/09/2025]. See the Terms

and-conditions) on Wiley Online Library for rules of use; OA articles are governed by the applicable Creative Common

a Bioinspired Design Sieve area Catalytic area ✓ Delivery sucrose ✓ Reduce energy barrier Microenvironment Companion cell for LiPSs conversion ✓ Provide sucrose Carbon wall ✓ Provide electron Confine tube Sieve tube ✓ Control LiPSs diffusion ✓ Control sucrose ✓ Inhibit LiPSs shuttle translocation channel-Fe<sub>SAC</sub> Plants sieve tubes



- (ii) Fe-S<sub>1</sub>N<sub>4</sub> coordination center
- (iii) In-situ catalytic conversion of CO, and O,

- (ii) V-S<sub>1</sub>N<sub>3</sub> asymmetry coordination center
- iii In-situ catalytic conversion of polysulfides

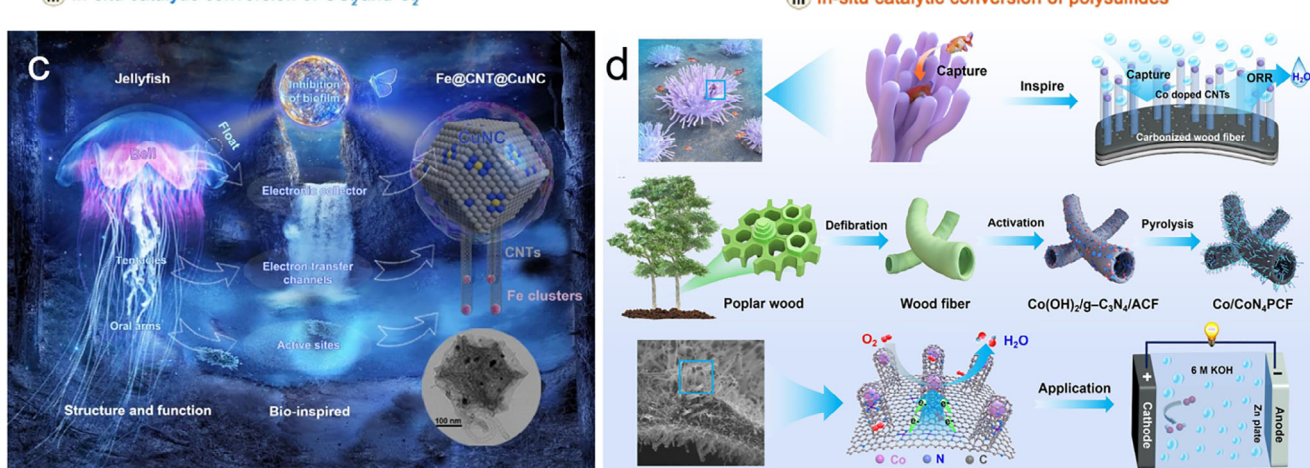


Figure 10. a) The biomimetic design strategy of a fully enclosed channel with a local trapping and catalytic microenvironment for Fe single atom cathodes (channel-Fe<sub>SAC</sub>). Reproduced with permission. [133] Copyright 2023, Wiley-VCH. b) Illustration of the biocatalytic function and benefits of alveolar tissue structure, and the suggested bioinspired carbon cathode featuring an interconnected porous construction and V-S<sub>1</sub>N<sub>3</sub> site for Li–S batteries with high efficiency and stability. Reproduced with permission. [137] Copyright 2024, Wiley-VCH. c) The jellyfish-inspired Fe@CNT@CuNC with Fe clusters and atomic Cu<sup>+</sup> sites connected by carbon nanotubes (CNTs). Reproduced with permission. [138] Copyright 2023, Springer Nature. d) Illustration of the synthesis process and characterization of the catalyst Co/CoN<sub>4</sub>PCF inspired by the shape and predation mechanism of sea anemones. The synthesis scheme, morphology, and application of Co/CoN<sub>4</sub>PCF. Reproduced with permission. [139] Copyright 2023, Elsevier.

1521495.6, Downloaded from https://advance.com/inerhards.wi.evj.com/oi/01/002/adma\_202502131 by HONG KONG POLYTECHICI UNIVERSITY HU IN HON, Wiley Online Library or [289-90252]. See the Terms and Conditions (https://oinlinelibrary.wiley.com/terms-a-d-conditions) on Wiley Online Library or rules of tase; OA articles are governed by the applicable Creative Commons I

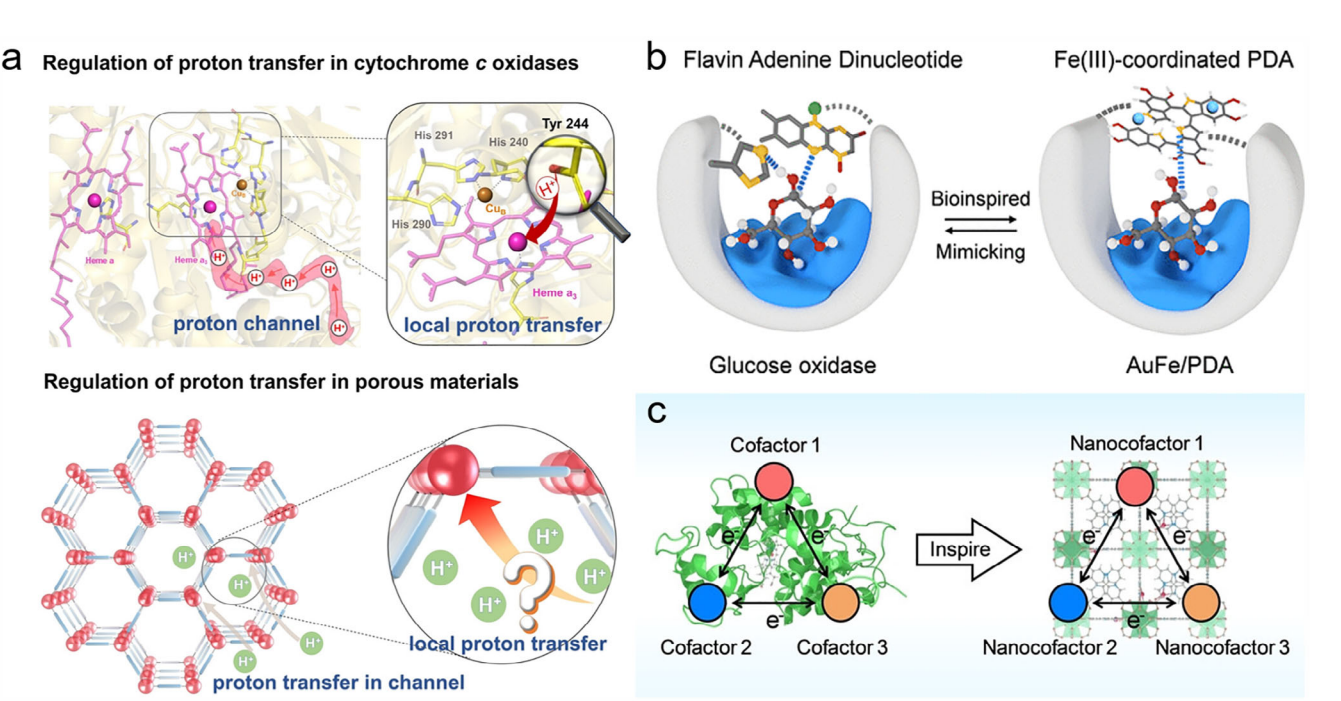


Figure 11. a) Regulation of proton transfer in cytochrome c oxidases (*CcOs*) and porous materials. Reproduced with permission.<sup>[142]</sup> Copyright 2024, Wiley-VCH. b) The AuFe/polydopamine (PDA) superparticles with photothermal-enhanced glucose oxidase-like activity. Reproduced with permission.<sup>[143]</sup> Copyright 2024, American Chemical Society. c) Schematic diagram of the synergistic effect of multiple nanocofactors. Reproduced with permission.<sup>[144]</sup> Copyright 2024, Wiley-VCH.

iron-sulfur clusters forming part of an electron transfer pathway (Figure 12a).<sup>[22,147]</sup> The catalytic site of NiFe hydrogenase comprises an organic metal group consisting of the NiFe dinuclear complex with nonprotein CN and CO ligands attached to the iron atom.<sup>[149]</sup> This complex plays a crucial role in hydrogen cleavage and proton transfer within the enzyme, facilitating interactions between the metal center and the surface of enzymes (Figure 12b).<sup>[150]</sup>

As mentioned above, these enzymes lack the required robustness and chemical stability, making hydrogenase-inspired SACs an excellent candidate. By precisely controlling the electronic structure of metal sites and their interactions with protons or hydrogen atoms, SACs can efficiently catalyze a range of proton reduction reactions using earth-abundant metals. Reversible synergistic activation processes are a key feature of biological enzymes. Leveraging the characteristics of electron transfer in redox mediators, reversible cofactor state changes, and macroscopic functional/structural changes, Hyeon's group have reported a highly

**Table 2.** Summary of bioinspired single-atom heterogeneous catalysts for electro-/photocatalysis by mimicking some natural enzymes.

Natural Enzymes	Enzymes Active Center	Bioinspired Catalyst	Catalysis Type
Hydrogenase	Ni/Fe	Ni/Fe/Ru/Cu single atom	HER
Nitrogenase	Fe/Mo	Fe/Mo/Ru single atom	NRR/NO <sub>3</sub> RR
Oxidase	Fe/Cu	Fe/Co/Cu/Se single atom	ORR
Dehydrogenase	Mo/W	Fe/Ni/Co/Cu single atom	CO <sub>2</sub> RR

active Cu single-atom-loaded TiO<sub>2</sub> photocatalyst (Figure 12c).<sup>[151]</sup> This catalyst exhibits reversible and synergistic photoactivation processes involving state control, reversible modulation of photoelectric properties, thus provides a platform for enhancing photocatalytic hydrogen production activity. The photoactivated cycle transfers from CT0 (inactive) to the photoexcited state (CT1 state), thereby generating electrons and holes, and resulting in a change in the copper atom's oxidation state (CT2 state) and local TiO<sub>2</sub> lattice distortion around the copper atom (CT3 state). This structural evolution in TiO2 significantly enhances photocatalytic hydrogen production activity. Subsequently, the active CT3 state can easily revert to the original inactive CT0 state in the presence of oxygen. This reversible copper single-atom interaction with TiO<sub>2</sub> validates the efficient catalytic transformation capability of these bioinspired SACs. Furthermore, it is interesting to draw inspiration from enzyme catalysis and create a hydrogenrich environment around the catalytic sites. Jiang's group have synthesized a series of single-atom Ru catalysts based on metalorganic frameworks (UiO-67), adjusting the distance between the hydrogen bond microenvironment and the Ru site by varying the position of the amino group (Figure 12d). [152] The NH<sub>2</sub> group can form unique hydrogen-bonded microenvironments with H<sub>2</sub>O and hence regulate the water concentration around the Ru site. The proximity of the Ru site to the hydrogen bond microenvironment facilitates charge transfer and water dissociation, significantly enhancing the hydrogen production activity. Additionally, controlling the loading of primary and secondary coordination spheres of Ni(II) unit points on UiO-67 metalorganic frameworks also regulates the hydrogen production microenvironment, promoting charge transfer dynamics and

15214095, 0, Downloaded from https://advanced.onlinelibrary.wiley.com/doi/10.1002/adma.202502131 by HONG KONG POL YTECHNIC UNIVERSITY HU NG HOM, Wiley Online Library on [28/09/2025]. See the Terms

conditions) on Wiley Online Library for rules of use; OA articles are governed by the applicable Creative Commo

#### Hydrogenase-inspired Heterogenous SACs for H<sub>2</sub> Evolution

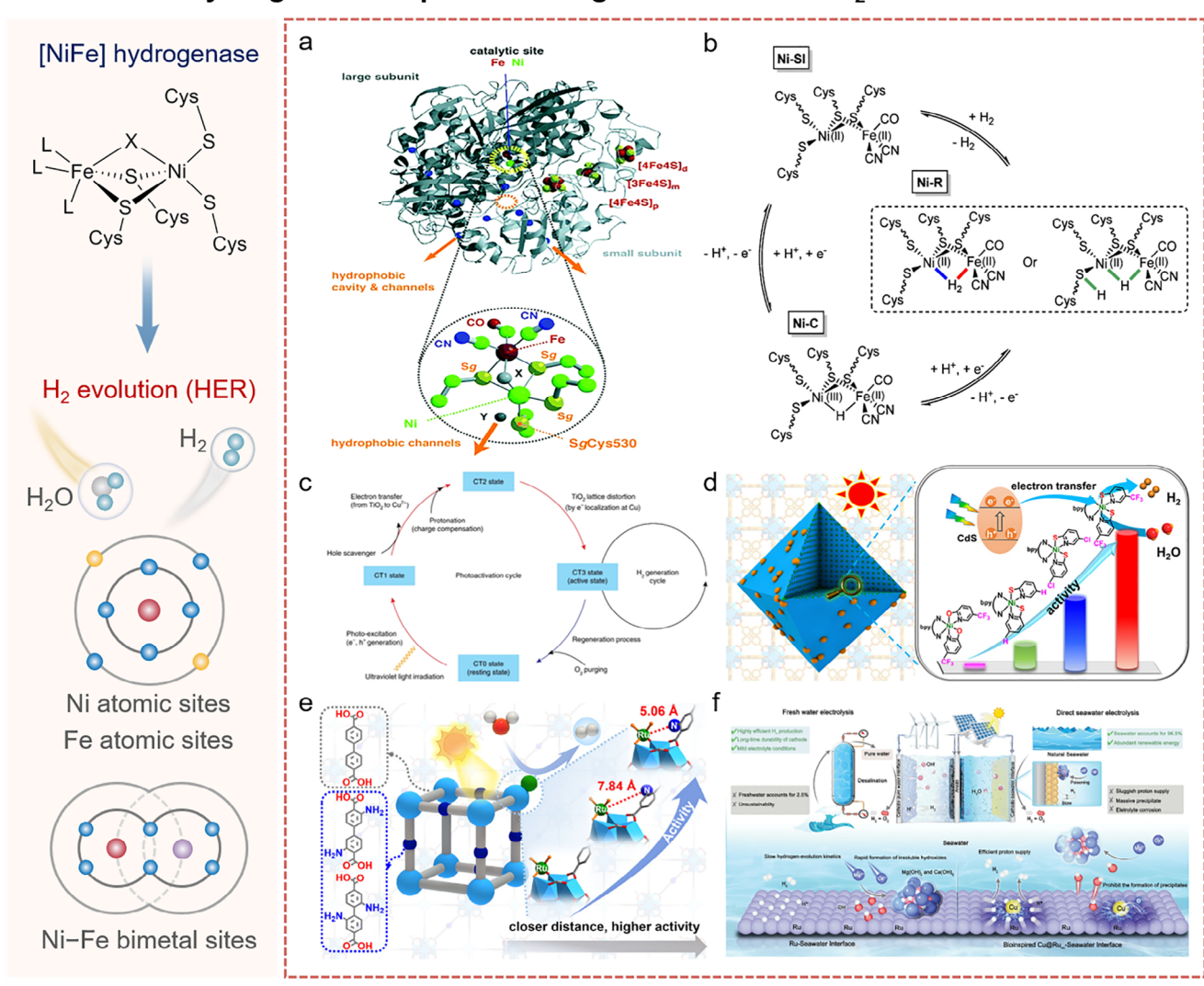


Figure 12. a) NiFe hydrogenases containing the catalytic center of Ni-Fe (dotted yellow circle) and iron-sulfur cluster and cavity and channels for molecular hydrogen transfer. Reproduced with permission. [132] Copyright 2002 Wiley-VCH. b) Postulated reversible H<sub>2</sub> oxidation reaction by [NiFe]hydrogenases. Adapted with permission. [150] Copyright 2006, Springer Nature. c) Photoactivation cycle of Cu/TiO2 in various states of photoactivation cycle. Reproduced with permission. [151] Copyright 2019, Springer Nature. d) Single Ni(II) sites onto UiO-67 framework deposited with CdS nanoparticles for photocatalytic H<sub>2</sub>. Reproduced with permission. [152] Copyright 2024, American Chemical Society. e) Inspired by enzymatic catalysis, MOF-based single-atom Ru<sub>1</sub> catalysts by modulating the distance between the hydrogen-bonding microenvironment and Ru<sub>1</sub> sites for photocatalytic hydrogen production. Reproduced with permission. [153] Copyright 2024, American Chemical Society. f) Schematic electrode design and Ru-seawater interface and bioinspired Cu@Runc-seawater interface (with low oxophilic and fast proton-transferring) for direct seawater hydrogen production. Reproduced with permission.[154] Copyright 2024 Wiley-VCH.

lowering activation barriers, resulting in activity modulation (Figure 12e). [153] Similarly, inspired by the bimetallic active sites in natural enzymes, Li's group have designed a Cu singleatom-modified Ru cluster on a porous carbon matrix as a cathode material for efficient hydrogen production from seawater (Figure 12f).[154] Benefiting from the microenvironment regulation provided by the electron-donating Cu element, Cu atoms are shown to promote the detachment of OH\* at the Ru-seawater interface. The Cu sites can also facilitate proton transfer and H<sub>2</sub> release through H\* overflow, achieving high current density in seawater electrolytes.

#### 3.2. Nitrogenase-Inspired Heterogenous SACs for Nitrogen-Based Chemicals Conversion

Nitrogenase is a metalloenzyme consisting of two protein components: the nitrogenase reductase NifH (also known as "Fe protein") and the catalytic NifDK (also known as "MoFe protein"). NifDK contains a unique molybdenum-iron-sulfur cluster called the M-cluster (or "FeMoco").[41] This enzyme plays a crucial role in nitrogen and CO2 reduction reactions, acting as a reductant and providing electron transfer. For instance, the Pcluster facilitates electron transfer between different components

15214095, 0, Downloaded from https://advanced.onlinelibrary.wiley.com/doi/10.1002/adma.202502131 by HONG KONG POLYTECHNIC UNIVERSITY HU NG HOM, Wiley Online Library on [28/09/2025]. See the Terms and Conditions (https://onlinelibrary.wiley.

and-conditions) on Wiley Online Library for rules of use; OA articles are governed by the applicable Creative Commons

#### Nitrogenase-inspired Heterogenous SACs for Value-added Chemicals

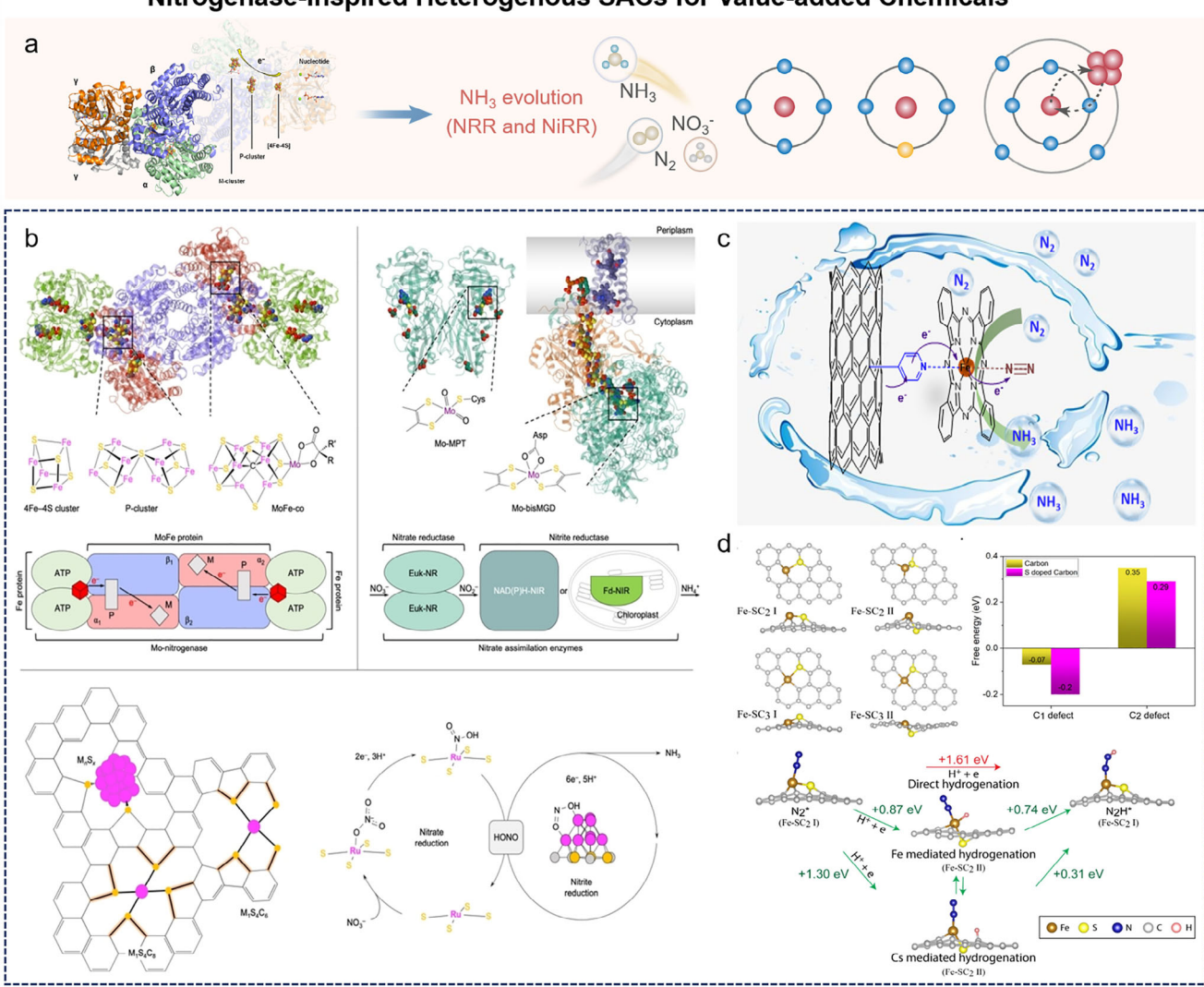


**Figure 13.** a) Crystal structure of the NifH:NifDK complex (PDB entry 1N2C), containing metalloclusters and the proposed direction of electron flow. NifD (green cartoon), NifK (blue cartoon), NifH (orange and gray cartoon), Fe, orange; S, yellow; C, gray. Adapted with permission.  $^{[14]}$  Copyright 2022, American Chemical Society. b) Molybdenum nitrogenase, and M–S–C catalyst. Reproduced with permission.  $^{[109]}$  Copyright 2024 Wiley-VCH. c) Biomimicking electrochemical NRR on FePc immobilized on pyridine-functionalized carbon nanotubes. Reproduced with permission.  $^{[155]}$  Copyright 2022, American Chemical Society. d) Proposed mechanisms of  $N_2$  hydrogenation on Fe–SC $_2$  by biomimicking nitrogenase. Reproduced with permission.  $^{[156]}$  Copyright 2022, American Chemical Society.

(Figure 13a). The nitrogenase-catalyzed nitrogen reduction process is highly complex, posing challenges in simulating its structure and nitrogen fixation process. Nitrogenase also catalyzes the reduction of protons to H<sub>2</sub>, transferring a portion of electron equivalents (or electron flux) to produce H<sub>2</sub> or other compounds in reactions with various substrates, including N<sub>2</sub> and CO<sub>2</sub>. To simplify reaction mechanisms and synthesize industrial catalysts more effectively, nitrogenase-inspired SACs have been developed, utilizing low-content transition metals like Ru, Fe, and Mo coordinated to donor ligands containing basic C, N, or S atoms to promote catalysis. For example, Wang's group developed a dual-component catalyst inspired by natural nitrogenase for NO<sub>3</sub><sup>-</sup> reduction reaction (NO<sub>3</sub>RR) to produce NH<sub>3</sub>, consisting of sulfur-doped carbon-supported Ru single atoms and

nanoparticles (Figure 13b).  $^{[109]}$  However, carrying out complex bonding/breaking steps to rearrange reactants into products, especially ammonia by solely mimicking the enzyme's active site is insufficient. It involves competitive adsorption of different intermediates and multiple electron and proton transfers, posing significant challenges in catalyst design. Through the design of this catalyst, a cascade catalytic mechanism was achieved with HONO as an intermediate for NH $_3$  production. N(V) reduction primarily occurs on isolated Ru SAs, followed by HONO migration to the Ru cluster surface to generate ammonia. Similarly, inspired by the vital role of iron in biological nitrogenase, well-defined iron-based catalysts have been developed for nitrogen reduction reaction (NRR). Lee's group has reported an electrocatalyst with Fe–N $_5$  active centers, where iron phthalocyanine



ADVANCED MATERIALS

www.advmat.de

(FePc) is uniformly immobilized on pyridine-functionalized carbon nanotubes (Figure 13c).[155] The pyridine groups covalently functionalized on the carbon nanotubes not only provide coordination for FePc bonding on the electrode surface but also serve as electron transfer relays to facilitate interfacial electron transfer between FePc and CNTs. By forming electron-deficient Fe centers, the FePc can catalyze the nitrogen reduction reaction. Similarly, Zhao's group have simulated the M-S bond in nitrogenase, inspired by understanding the metal-sulfur bonds in nitrogenase.[156] By embedding sulfur into mesoporous carbon matrices to modulate the iron's electronic structure, the performance of NRR could be improved due to enhancement of electron transfer rate and flexibility of the Fe-S-C bonds (Figure 13d). The locally charged density points can enhance N<sub>2</sub> interaction, achieved through the Fe-S-C bond formation. Sulfur, as a heteroatom, can coordinate with transition metals and act as a bridge between metal and carbon, creating local high charge density points that serve as centers for N2 adsorption and activation. Sulfur tends to adsorb H, promoting consecutive hydrogenation of activated nitrogen atoms, leading to enhanced nitrogen reduction. Both the simulation of active sites and the regulation of microenvironments demonstrate the successful emulation of enzymatic activities through single-atom catalysis.

### 3.3. Oxidase-Inspired Heterogenous SACs for Oxygen-Based Chemicals Conversion

Oxygen reduction is fundamental to aerobic respiration and serves as a key reaction in industrial applications such as fuel cells. The ORR is a multielectron, multistep reaction involving various reaction intermediates and proton-coupled electron transfer steps before the O-O bond cleavage. [98,157,158] The reaction mechanism can be categorized into two electron systems and four electron systems. In acidic media, the four-electron pathway directly produces H<sub>2</sub>O, while the two-electron pathway results in H<sub>2</sub>O<sub>2</sub>. In alkaline media, the four-electron pathway generates OH-, whereas the two-electron pathway produces HO2as an intermediate product. High-efficiency catalytic systems like CcO-heme-copper oxidases selectively reduce O2 to H2O under the catalysis of iron and copper (Figure 14a,b).[159-161] Similarly, multicopper oxidases like laccase activate the O-O bond, facilitating multielectron/multiproton chemistry and/or selectively producing H<sub>2</sub>O (Figure 14b).<sup>[162]</sup> Drawing inspiration from the mechanisms of these enzymes, researchers have developed a range of single-atom heterogeneous catalytic systems for oxygen reduction applications. For example, Shi's group have reported the synthesis of Cu/Fe-doped single-atom catalysts inspired by natural hemoglobin-copper oxidase (Figure 14c).[163] By adjusting the central metal atom, coordinating atoms, and environmental atoms, the electrocatalytic ORR activity could be enhanced. The research group further demonstrated that the biomimetic heterobimetallic Cu-Fe center exhibits a good balance of optimal adsorption of oxygenated species at the active site and significant synergistic effects between the two metal atoms, which contribute to the enhanced catalytic activity. Inspired by the unique second spheres near the active sites of natural enzymes, Duan's group has synthesized single Co-N<sub>4</sub>

atomic catalysts with pendant amine groups in the second sphere (Figure 14d).[164] This configuration allows modulation of the SAC's microenvironment and catalytic reactivity, switching the selectivity of the oxygen reduction reaction from the 4e<sup>-</sup> pathway to the 2e<sup>-</sup> pathway under acidic conditions. The introduced pendant amine acts as a proton relay, facilitating the protonation of \*O2 to \*OOH at the Co-N4 active site and promoting the selective formation of H<sub>2</sub>O<sub>2</sub> up to 97%. Similarly, Liu's group has reported a novel biomimetic ORR catalyst, a multinuclear copper complex, inspired by the effective catalysis of ORR by laccase's multicopper active sites (Figure 14e).[165] By introducing graphene as a fixed polymer base, electronic transfer between the catalyst and the carrier material is facilitated. The dinuclear Cu complex, anchored on the rGO surface with covalently grafted TADPy ligands, exhibits high selectivity for the 4e<sup>-</sup> reduction process and good stability in alkaline environments. Furthermore, Co-corrole-based porous organic polymers improve proton transfer for electrocatalytic oxygen reduction reaction, which can be correlated to how enzymes transfer external protons to the buried active sites.<sup>[142]</sup> These studies vividly demonstrate the potential of single-atom heterogeneous catalysis in mimicking biological enzymes by simulating the synergistic interactions between active sites, regulating the microenvironment around the sites, and understanding proton-electron interactions and transfer mechanisms. Besides the natural oxidases, Wang's group also garner the inspiration from glutathione peroxidase (selenoenzyme) which is capable of scavenging ROS in biological organisms.[166] They fabricate a biomimetic single atomic selenium (Se) site with carbon moiety (Se-C) to achieve selective ORR performance via a consecutive 2 + 2 electron pathway.

## 3.4. CO and Formate Dehydrogenase-Mimicked Heterogenous SACs for CO<sub>2</sub>RR

In nature, carbon monoxide dehydrogenases (CODHs) participate in the reversible oxidation of carbon monoxide and the reduction of carbon dioxide. These enzymes are primarily molybdenum-based and catalyze the aerobic oxidation of CO (resulting in CO2 release), though some anaerobic bacteria and archaea containing CODHs with nickel, iron, and sulfur clusters (Figure 15a).[168] Similarly, formate dehydrogenases (FDHs) are enzymes that catalyze the reversible extraction of two electrons and one proton from formate to produce carbon dioxide. FDHs feature Mo and W as the primary metal active centers coordinated by dithiolene groups from a protein-derived selenocysteine or cysteine ligand, along with a sixth ligand believed to be a sulfide ligand (Figure 15b). [41] In this context, we would focus on the biomimetic applications of dehydrogenases in the reduction of CO<sub>2</sub> For example, Jiang's group have introduced a novel Fe-Ni-N-C catalyst featuring adjacent Fe and Ni singleatom pairs to mimic Ni-Fe CODH activity (Figure 15c). [169] The close interaction between the neighboring single Fe and Ni atoms results in the high activation of the Ni atom by the Fe atom through nonbonding interactions. This synergistic effect between the sites significantly enhances catalytic performance, surpassing the efficiency of individual sites. The precise construction of adjacent single-atom sites in SACs enables

15214059. D. Downloaded from thtps://advance.onlinelibrary.wiley.com/oi/01/01/02/adna.2025/231 by HONG KONG POLYTECHNIC UNIVERSTY HU NG HOM, Wiley Online Library on (128/09/2025). See the Terms and Conditions (https://onlinelibrary.wiley.com/emrs-and-conditions) on Wiley Online Library for rules of use; OA articles as a governed by the applicable Creative Commons

#### Oxidase-inspired Heterogenous SACs for Oxygen-based Chemicals Conversion

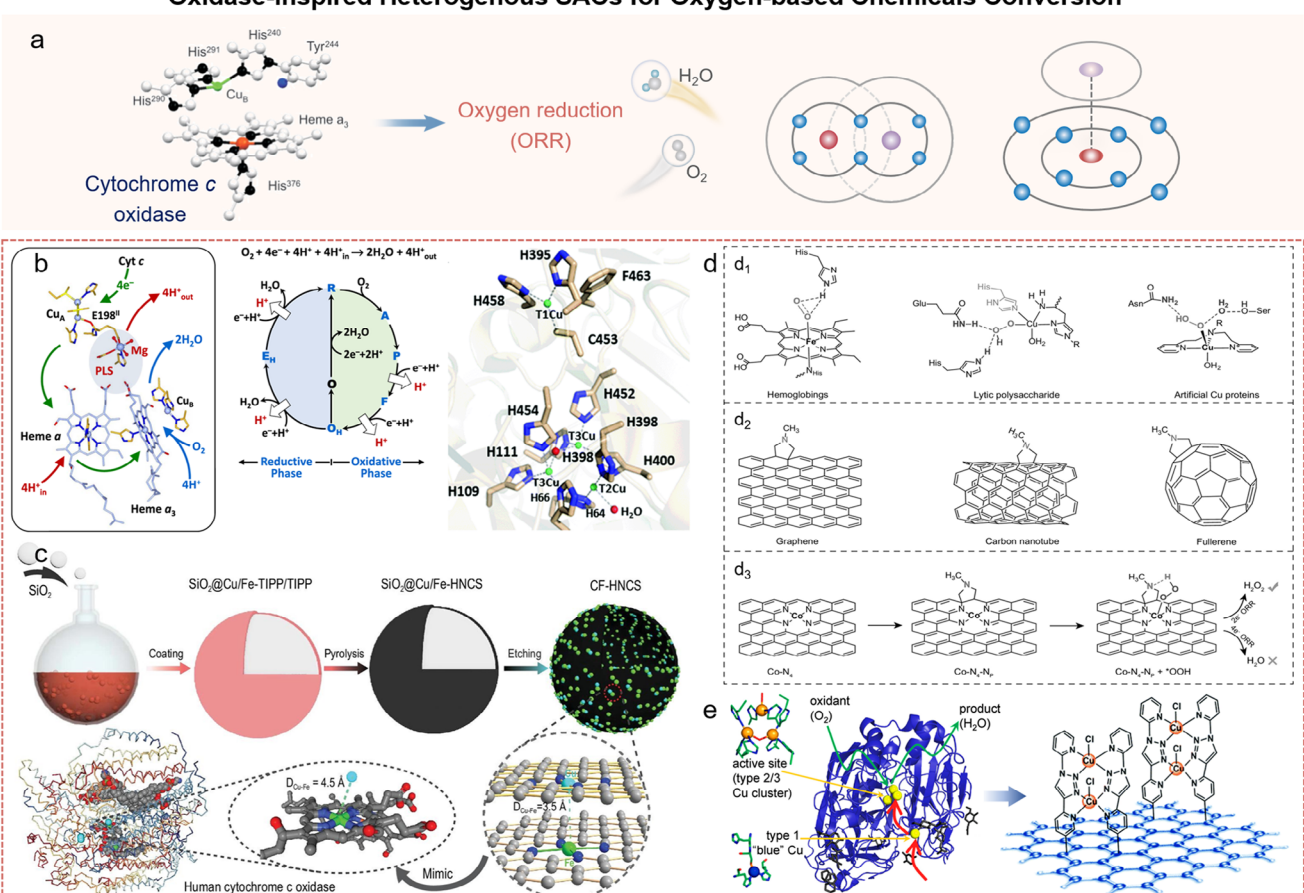


**Figure 14.** a) Crystal structure of CcO from the bovine heart and the oxidase-inspired heterogenous SACs for oxygen-based chemicals conversion. Adapted with permission. CcO model with the overall ORR mechanism. Reproduced under the terms of the CC-BY Creative Commons Attribution 4.0 International License. CcO model with the overall ORR mechanism. Reproduced under the terms of the CC-BY Creative Commons Attribution 4.0 International License. CcO model with permission. CcO mod

efficient molecular catalysis, achieving a Faradaic efficiency of 96.2% in CO<sub>2</sub> electrochemical reduction. Similarly, inspired by carbon monoxide dehydrogenase, Yue's group have designed a covalent organic framework (THD-COF) featuring bioinspired N,S-coordination sites and single Co atoms (Figure 15d).[170] The THD-COF matrix and Co active centers significantly enhanced CO2 adsorption activation and charge separation kinetics, reducing the energy barrier for critical \*COOH intermediate formation. The N, S-Co sites effectively gather photoinduced electrons and immobilize \*COOH, enhancing CO2 activation and conversion efficiency. Furthermore, Zhang's group have developed a bioinspired photocatalyst inspired by the catalytic ability and specificity principles of formate dehydrogenase (Figure 15e).[122] This synthetic photocatalyst exhibited outstanding efficiency in CO<sub>2</sub>-to-ethanol photoelectrochemical reduction. The spatially functional NH<sub>2</sub>···Cu-Se(-Zn) structure in ZnSe

colloidal quantum wells closely mimics the interaction between the active site and surrounding coordination spheres in enzymatic catalysis. This biomimetic design facilitates CO2 adsorption and activation, proton and photo-induced electron transfer, stabilization of generated \*CO and \*CHO intermediates, ultimately leading to the asymmetric coupling of C-C bonds to produce ethanol. Additionally, Ding's group have demonstrated the activity of [NiS<sub>4</sub>] sites in mimicking formate dehydrogenase and carbon monoxide dehydrogenase (Figure 15f).[171] The utilization of redox-active nickel dithiolene-based MOF catalysts with unsaturated [NiS<sub>4</sub>] sites lead to a remarkable increase in the conversion rate and Faradaic efficiency of HCOOproduction. This unprecedented effect is attributed to the impact of the [NiS<sub>4</sub>] sites as CO<sub>2</sub> binding sites and efficient catalytic centers for CO2 electroreduction, mimicking enzyme-like activities.

www.advmat.de

15214095, 0, Downloaded from https://adanceed.onlinelibrary.wiley.com/doi/10.1002/adma.202502131 by HONG KONG POL YTECHNIC UNIVERSITY HU NG HOM, Wiley Online Library on [28/09/2025]. See the Terms and Conditions (https://onlinelibrary.wiley.com/doi/10.1002/adma.202502131 by HONG KONG POL YTECHNIC UNIVERSITY HU NG HOM, Wiley Online Library on [28/09/2025]. See the Terms and Conditions (https://onlinelibrary.wiley.com/doi/10.1002/adma.202502131 by HONG KONG POL YTECHNIC UNIVERSITY HU NG HOM, Wiley Online Library on [28/09/2025]. See the Terms and Conditions (https://onlinelibrary.wiley.com/doi/10.1002/adma.202502131 by HONG KONG POL YTECHNIC UNIVERSITY HU NG HOM, Wiley Online Library on [28/09/2025]. See the Terms and Conditions (https://onlinelibrary.wiley.com/doi/10.1002/adma.202502131 by HONG KONG POL YTECHNIC UNIVERSITY HU NG HOM, Wiley Online Library on [28/09/2025]. See the Terms and Conditions (https://onlinelibrary.wiley.com/doi/10.1002/adma.202502131 by HONG KONG POL YTECHNIC UNIVERSITY HU NG HOM, Wiley Online Library on [28/09/2025]. See the Terms and Conditions (https://onlinelibrary.wiley.com/doi/10.1002/adma.202502131 by HONG KONG POL YTECHNIC UNIVERSITY HU NG HOM. Wiley Online Library on [28/09/2025]. See the Terms and Conditions (https://onlinelibrary.wiley.com/doi/10.1002/adma.202502131 by HONG KONG POL YTECHNIC UNIVERSITY HU NG HOM. Wiley Online Library on [28/09/2025]. See the Terms and Conditions (https://onlinelibrary.wiley.com/doi/10.1002/adma.202502131 by HONG KONG POL YTECHNIC UNIVERSITY HU NG HOM Wiley Online Library on [28/09/2025]. See the Terms and Conditions (https://onlinelibrary.wiley.com/doi/10.1002/adma.202502131 by HONG KONG POL YTECHNIC UNIVERSITY HU NG HOM Wiley Online Library on [28/09/2025]. See the Terms and Conditions (https://onlinelibrary.wiley.com/doi/10.1002/adma.202502131 by HONG KONG POL YTECHNIC UNIVERSITY HU NG HOM Wiley Online Library on [28/09/2025].

and-conditions) on Wiley Online Library for rules of use; OA articles are governed by the applicable Creative Commons

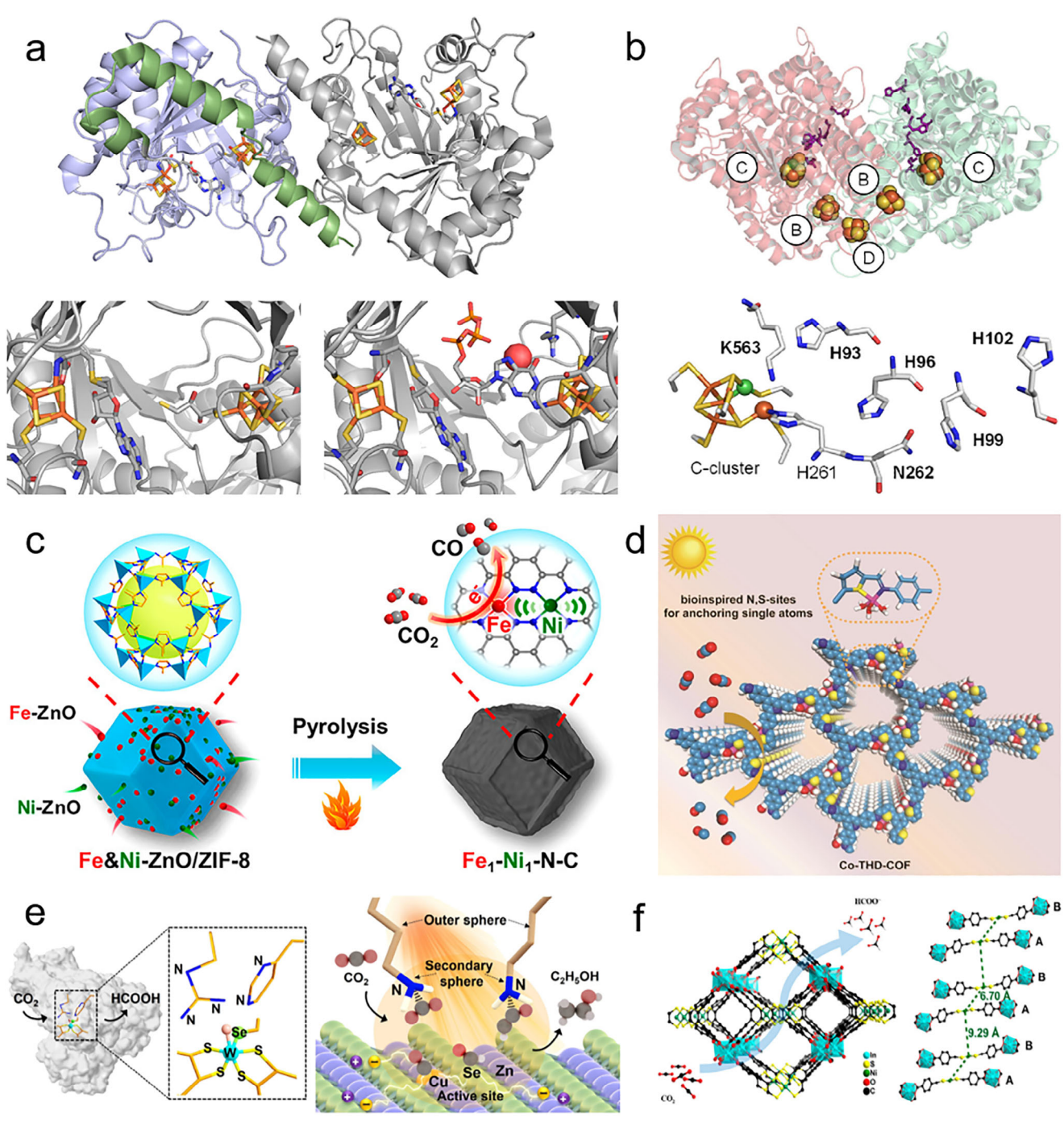


Figure 15. a) The structure of MoaA from *S. aureus*. Top, the dimeric enzyme, with the N- and C-terminal domains of the subunit on the left shaded in blue and green, respectively. Bottom left, S-adenosylmethionine bound to the N-terminal [4Fe-4S] cluster and dithiothreitol bound to the C-terminal [4Fe-4S] (PDB entry 1TV8). Bottom right, GTP bound to the C-terminalcluster, and methionine bound at the N-terminal cluster. Reproduced with permission. [168] Copyright 2014, American Chemical Society. b) Structure of CODH: *Ch*CODH II (PDB entry 1SU8). The spheres: inorganic cofactors. Labeled C-cluster: cofactor. The purple: putative proton transfer. Fe, orange; Ni, green; S, yellow; C, gray; O, red; N, blue. Reproduced with permission. [41] Copyright 2022, American Chemical Society. c) Fe<sub>1</sub>–Ni<sub>1</sub>–N–C catalyst with neighboring Fe and Ni single-atom pairs decorated on nitrogen-doped carbon support for electrocatalytic reduction of CO<sub>2</sub>. Reproduced with permission. [169] Copyright 2021, American Chemical Society. d) Bioinspired single Co atoms coordinated with N, S-sites to create Co-THD-COF, which photocatalyzed CO<sub>2</sub> conversion to CO. Reproduced with permission. [170] Copyright 2024, Elsevier. e) Left: Structure of FDH, containing the outer protein scaffold and inner sphere of active site consists of W in coordination with selenocysteine. Right: The bioinspired SACs structure of Cu<sub>0.15</sub>/ZnSe QWs, and the inner active site: Cu–Se(–Zn), secondary coordination sphere: amino head of vicinal OA and OLA ligands, and the outer coordination spheres: the ligand hydrocarbon chains. Reproduced with permission. [172] Copyright 2024, the American Association for the Advancement of Science. f) Simplified diagram of CO<sub>2</sub>RR and the [NiS<sub>4</sub>] sites. Reproduced with permission. [171] Copyright 2021, American Chemical Society.

com/doi/10.1002/adma.202502131 by HONG KONG POLYTECHNIC UNIVERSITY HU NG HOM, Wiley Online Library on [28/09/2025]

on Wiley Online Library for rules of use; OA articles are governed by the applicable Creative Commons

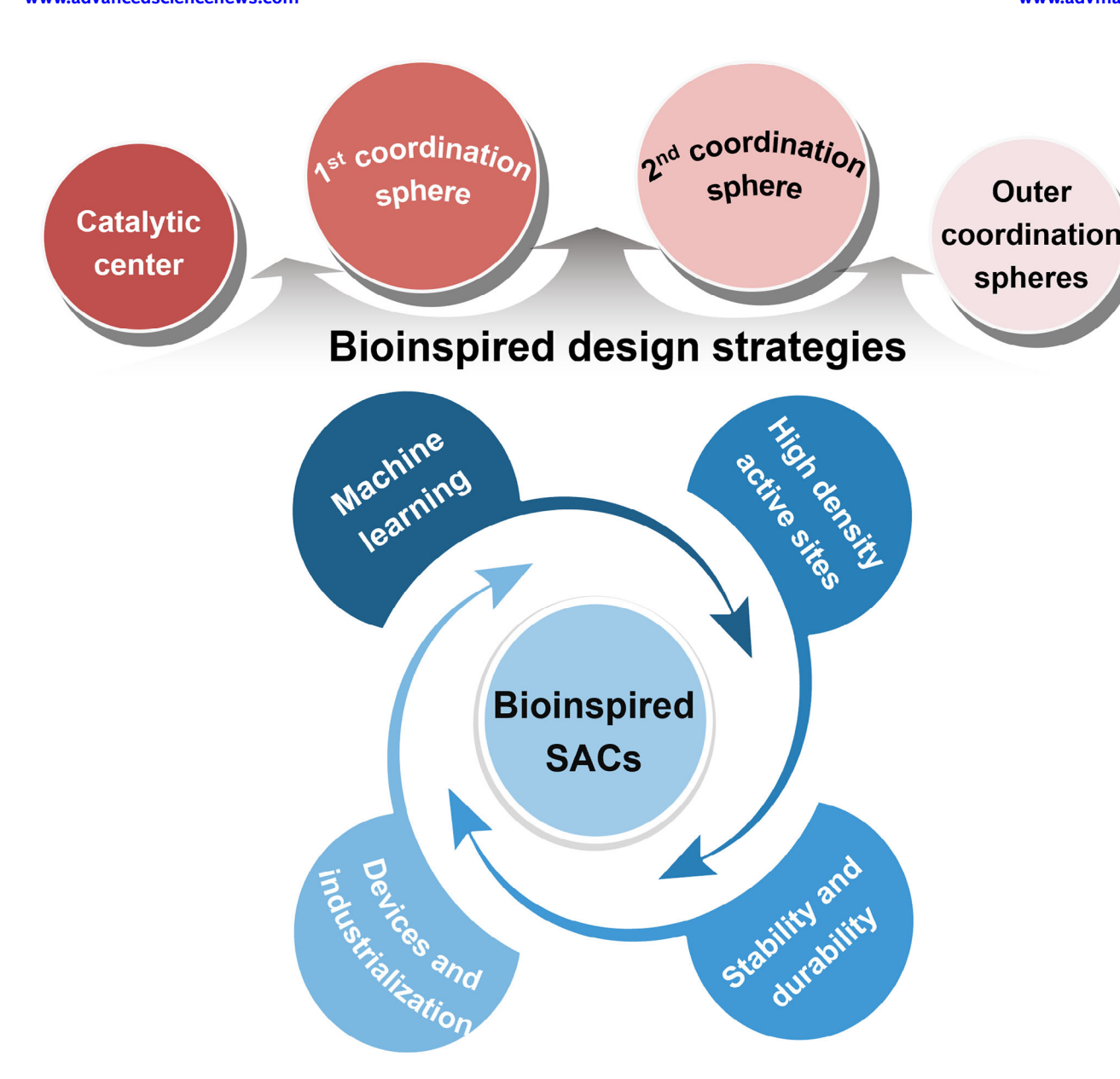


Figure 16. The schematic illustration of great opportunities for the development of bioinspired SACs.

#### 4. Conclusion and Perspective

The development of engineering strategies plays a fundamental role in designing well-defined heterogenous SACs. In this review, we can see that bioinspired design strategies have been successfully established from the inner single metal centers to the outer microenvironment to fabricate complex SACs. The practical applications of those bioinspired SACs in heterogeneous electro-/photocatalysis have been achieved. Despite tremendous progress have been witnessed, bridging the gap from homogenous biocatalysis to heterogenous catalysis still faces foreseeable challenges. With the development of artificial intelligence and synthetic strategies and advancement in characterization techniques, there are ample opportunities to further

design and optimize the SAC structures for various applications (Figure 16).

#### 4.1. Machine Learning

Machine learning (ML) is a branch of artificial intelligence (AI) that serves as an emerging and promising tool in materials science, assisting in resource-intensive experimental and computational tasks through statistical models and algorithmic systems. ML models information based on provided data and offers potential solutions to address these tasks. For instance, for in-depth studies of SAC materials, ML can play a crucial role in predicting material performance without the need for DFT.



ADVANCED MATERIALS

www.advmat.de

Furthermore, if the material's structure and its local environment are provided, ML models will learn potential target properties. Additionally, the emergence of bioinspired ML techniques enables the invention of solutions to mitigate human errors in complex systems. Many technological innovations are inspired by insights drawn from natural systems. These methods represent an interdisciplinary and promising approach that integrates biological activities into machines to enhance their intelligence, mimicking nature to serve various goals such as designing complex compounds, detecting, and converting energy. Therefore, the potential of bioinspired computing lies in its cost-effective and sustainable approach to addressing common problems. For example, utilizing bioinspired machine learning to study the structure-activity relationship of SACs is a promising strategy. This can potentially shorten the lifespan of design and synthesis, as well as reduce chemical and energy consumption, as current SACs research relies on a trial-and-error processes. The formation mechanism of SACs in thermal conversion processes and the structure-catalysis relationship are not fully understood. Due to limitations in time and computational resources, traditional DFT calculations are not suitable for screening a large number of models. With the rapid development of software and hardware, data analysis based on ML and quantitative structure-activity relationships is convenient and reliable. It can establish correlations between descriptors such as catalyst properties, operating and reactor parameters, and catalytic performance.[172,173] These advanced tools enable high-throughput direct prediction of catalytic performance, allowing for accelerated screening and discovery of on-demand SACs under conditions close to reality.[174]

#### 4.2. High Density Active Sites in Bioinspired SACs

The catalytic activity of a catalyst is closely related to the site density. The metal content in natural metalloenzymes typically ranges from 0.05 to 5 wt%, depending on the metal type and the structural configuration of the enzyme. [175] Although metals constitute a small proportion, they are critically essential for enzymatic activity. Bioinspired SACs with precise structures and high site loading can modulate catalytic performance by altering the electronic structure of the metal center such as changing the type and number of metals, metal coordination number, doping of thermal atoms, etc. However, achieving the desired atomic structure precisely in experiments poses challenges. Information obtained through ML screening can significantly guide the structure of active sites in catalysts and provide insights into synthetic methods based on the learned information. For instance, hightemperature annealing rapidly produces high-density and stable SACs catalysts but may lead to unpredictable structural changes in the material, making it difficult to obtain the desired atomic active sites in the microenvironment. Wet chemistry methods can address microenvironmental issues related to chemical sites precisely, but ensuring stability and site density of active sites can be challenging. To address this, thoughtful modulation of various parameters to understand the role of each component or develop new methods is crucial. Typically, achieving the density of active sites above 5 wt% in SACs is extremely challenging. This limitation hinders their potential for industrial applications. Some relevant studies have reported SACs with loadings exceeding 20 wt%, which is widely recognized to enhance catalytic activity and stability. [176,177] Those SACs are generally synthesized with strictly controlled protocols, where the ultrahigh-density anchoring sites existed on the support with strong metal-support interaction. These characteristics offer additional insights into the further development of bioinspired design strategies towards heterogenous SACs. Various parameters will play a crucial role in improving the metal content and preventing aggregation of single metal sites. These parameters may include porosity, size, and dimensions of the support, the interaction between the substrate and atomic sites, interactions of atomic sites, and changes in the microenvironment of atomic sites during the reaction process. Therefore, it is necessary to design specific structures under the guidance of current synthetic strategies to meet specific catalytic tasks and achieve maximal catalytic activity.

#### 4.3. Selectivity and Durability

Structural biomimicry is essential for replicating the functionality of enzymes, as their substrate specificity arises from evolutionary optimization of active-site geometry, electronic states, and dynamic interactions with substrates. While bioinspired SACs aim to mimic enzyme-like selectivity by designing atomically dispersed metal centers with tailored coordination environments, current synthetic strategies still lack the atomic-level structural fidelity of natural enzymes. Enzymes achieve specificity through precisely positioned amino acid residues, hydrogen-bonding networks, and conformational flexibility and these features are not yet fully replicated in SACs.

Studying the relationship between material stability and catalytic performance, as well as scaling up applications, is crucial in the field of catalysis. Particularly for SACs, which offer a promising alternative to noble metal-based catalysts due to their inherent geometric and electronic advantages. SACs are prone to dissolution, detachment, aggregation, and poisoning under varying reaction conditions such as strong acid or base solutions and gas environments. These factors can lead to decreased activity or deactivation of the catalyst, impacting its long-term durability. Strategies such as strong metal-support interactions, spatial confinement, self-adaptive single atoms, and reversible atomic valence states can help to stabilize the active sites.[178] Therefore, the efficiency of reusing SACs catalysts is important. Further research is needed to retain the separated metal active sites during and after the regeneration process. Even with superior stability of catalyst sites, considerations must be made for potential losses during the reaction process. This relies on the overall catalyst design, such as self-supported designs and the use of gas diffusion layers. Thus, synthesizing SACs with excellent catalytic stability, resistance to harsh catalytic conditions, and appropriate device design is crucial for their large-scale industrial applications.

#### 4.4. Devices and Industrialization

The large-scale production of SACs with a simple strategy is important for practical applications. While some effective methods have been developed to synthesize SACs with high loading

and/or thermal stability, reports on large-scale production of stable, high-loading SACs remain scare. Therefore, there is an urgent need to develop simple and versatile methods for the largescale production of SACs, which holds crucial implications for their practical applications. Considering that the minimum industrial or commercial production scale for catalysts is around 100 kg, the reported synthesis scales currently fall far short of industrial-scale production. In recent years, there has been increasing focus on the large-scale synthesis of SACs which is the final and critical step in industrial applications but has been consistently underestimated in the research community. Therefore, recognizing scaling-up challenges in the early stages of catalyst preparation can expedite the industrialization of new catalytic materials. Laboratory-prepared SACs may differ significantly from technical catalysts tailored for large-scale industrial operations. Research catalysts are designed to screen various materials in the initial stages of catalyst development to enhance catalytic activity. In contrast, technical catalyst manufacturing focuses on evaluating their industrial application potential using cost-effective technical-grade reagents and additives to improve catalyst properties for long-term operation under harsh conditions. Achieving a balance between cost-effectiveness and efficiency is crucial in this process. Therefore, close collaboration between academia and industry is key to advancing SACs towards commercial catalysts and providing insights into these processes, facilitating the development of optimized large-scale synthetic methods.

#### Acknowledgements

Y.W. and G.J. contributed equally to this work. K.-Y.W. acknowledges the support from the Hong Kong Innovation and Technology Commission to the State Key Laboratory of Chemical Biology and Drug Discovery and the Patrick S. C. Poon Endowed Professorship. Y.W. acknowledges the support from the National Youth Talent Program and the Fundamental Research funds for the Central Universities (3072025CFJ1007).

#### **Conflict of Interest**

The authors declare no conflict of interest.

#### Keywords

bioinspired strategy, electrocatalysis, heterogeneous catalyst, photocatalysis, single-atomic-site catalyst

Received: January 31, 2025 Revised: May 6, 2025 Published online:

- [1] S. Chu, A. Majumdar, Nature 2012, 488, 294.
- [2] S. Chu, Y. Cui, N. Liu, Nat. Mater. 2017, 16, 16.
- [3] M. K. Debe, Nature 2012, 486, 43.
- [4] K. Maeda, K. Teramura, D. Lu, T. Takata, N. Saito, Y. Inoue, K. Domen, *Nature* 2006, 440, 295.
- [5] C. Vogt, B. M. Weckhuysen, Nat. Rev. Chem. 2022, 6, 89.
- [6] K. Qi, Y. Zhang, N. Onofrio, E. Petit, X. Cui, J. Ma, J. Fan, H. Wu, W. Wang, J. Li, J. Liu, Y. Zhang, Y. Wang, G. Jia, J. Wu, L. Lajaunie, C. Salameh, D. Voiry, Nat. Catal. 2023, 6, 319.

- [7] G. Jia, Y. Wang, M. Sun, H. Zhang, L. Li, Y. Shi, L. Zhang, X. Cui, T. W. B. Lo, B. Huang, J. C. Yu, J. Am. Chem. Soc. 2023, 145, 14133
- [8] B. Qiao, A. Wang, X. Yang, L. F. Allard, Z. Jiang, Y. Cui, J. Liu, J. Li, T. Zhang, Nat. Chem. 2011, 3, 634.
- [9] X.-F. Yang, A. Wang, B. Qiao, J. Li, J. Liu, T. Zhang, Acc. Chem. Res. 2013, 46, 1740.
- [10] Z. Li, S. Ji, Y. Liu, X. Cao, S. Tian, Y. Chen, Z. Niu, Y. Li, Chem. Rev. 2020, 120, 623.
- [11] X. Cui, W. Li, P. Ryabchuk, K. Junge, M. Beller, *Nat. Catal.* **2018**, *1*,
- [12] Š. Kment, A. Bakandritsos, I. Tantis, H. Kmentová, Y. Zuo, O. Henrotte, A. Naldoni, M. Otyepka, R. S. Varma, R. Zbořil, Chem. Rev. 2024, 124, 11767.
- [13] Z.-W. Deng, Y. Liu, J. Lin, W.-X. Chen, Rare Met. 2024, 43, 4844.
- [14] T. Tang, Z. Wang, J. Guan, Exploration 2023, 3, 20230011.
- [15] Y. Wang, H. Su, Y. He, L. Li, S. Zhu, H. Shen, P. Xie, X. Fu, G. Zhou, C. Feng, D. Zhao, F. Xiao, X. Zhu, Y. Zeng, M. Shao, S. Chen, G. Wu, J. Zeng, C. Wang, Chem. Rev. 2020, 120, 12217.
- [16] C. Gao, J. Low, R. Long, T. Kong, J. Zhu, Y. Xiong, Chem. Rev. 2020, 120, 12175.
- [17] C. Jia, Q. Sun, R. Liu, G. Mao, T. Maschmeyer, J. J. Gooding, T. Zhang, L. Dai, C. Zhao, Adv. Mater. 2024, 36, 2404659.
- [18] Y. Wang, D. Wang, Y. Li, Adv. Mater. 2021, 33, 2008151.
- [19] B. B. Sarma, F. Maurer, D. E. Doronkin, J.-D. Grunwaldt, Chem. Rev. 2023, 123, 379.
- [20] U. T. Bornscheuer, G. W. Huisman, R. J. Kazlauskas, S. Lutz, J. C. Moore, K. Robins, *Nature* 2012, 485, 185.
- [21] J. Barrio, A. Pedersen, S. Favero, H. Luo, M. Wang, S. C. Sarma, J. Feng, L. T. T. Ngoc, S. Kellner, A. Y. Li, A. B. Jorge Sobrido, M.-M. Titirici, Chem. Rev. 2023, 123, 2311.
- [22] P. Trogadas, M.-O. Coppens, Chem. Soc. Rev. 2020, 49, 3107.
- [23] P. Trogadas, L. Xu, M.-O. Coppens, Angew. Chem., Int. Ed. 2024, 63, 2023 14446.
- [24] X. Li, L. Liu, X. Ren, J. Gao, Y. Huang, B. Liu, Sci. Adv. 2020, 6, abb6833.
- [25] W. Song, C. Xiao, J. Ding, Z. Huang, X. Yang, T. Zhang, D. Mitlin, W. Hu, Adv. Mater. 2024, 36, 2301477.
- [26] H. Wang, T. Yang, J. Wang, Z. Zhou, Z. Pei, S. Zhao, Chem 2024, 10, 48.
- [27] Y. Qu, Z. Li, W. Chen, Y. Lin, T. Yuan, Z. Yang, C. Zhao, J. Wang, C. Zhao, X. Wang, F. Zhou, Z. Zhuang, Y. Wu, Y. Li, *Nat. Catal.* 2018, 1, 781.
- [28] M.-X. Chen, M. Zhu, M. Zuo, S.-Q. Chu, J. Zhang, Y. Wu, H.-W. Liang, X. Feng, Angew. Chem., Int. Ed. 2020, 59, 1627.
- [29] G.-F. Han, F. Li, A. I. Rykov, Y.-K. Im, S.-Y. Yu, J.-P. Jeon, S.-J. Kim, W. Zhou, R. Ge, Z. Ao, T. J. Shin, J. Wang, H. Y. Jeong, J.-B. Baek, Nat. Nanotechnol. 2022, 17, 403.
- [30] K. Khan, T. Liu, M. Arif, X. Yan, M. D. Hossain, F. Rehman, S. Zhou, J. Yang, C. Sun, S.-H. Bae, J. Kim, K. Amine, X. Pan, Z. Luo, Adv. Energy Mater. 2021, 11, 2101619.
- [31] Y. Zhang, J. Zhao, H. Wang, B. Xiao, W. Zhang, X. Zhao, T. Lv, M. Thangamuthu, J. Zhang, Y. Guo, J. Ma, L. Lin, J. Tang, R. Huang, Q. Liu, Nat. Commun. 2022, 13, 58.
- [32] S. Shen, Q. Li, H. Zhang, D. Yang, J. Gong, L. Gu, T. Gao, W. Zhong, Adv. Mater. 2025, 37, 2500595.
- [33] Y. Wang, V. K. Paidi, W. Wang, Y. Wang, G. Jia, T. Yan, X. Cui, S. Cai, J. Zhao, K.-S. Lee, L. Y. S. Lee, K.-Y. Wong, *Nat. Commun.* 2024, 15, 2239.
- [34] G. Jia, M. Sun, Y. Wang, Y. Shi, L. Zhang, X. Cui, B. Huang, J. C. Yu, Adv. Funct. Mater. **2022**, *32*, 2206817.
- [35] T. Zhang, X. Yang, J. Jin, X. Han, Y. Fang, X. Zhou, Y. Li, A. Han, Y. Wang, J. Liu, Adv. Mater. 2024, 36, 2304144.
- [36] Z. Gao, A. Li, X. Liu, M. Peng, S. Yu, M. Wang, Y. Ge, C. Li, T. Wang, Z. Wang, W. Zhou, D. Ma, *Nature* 2025, 638, 690.



www.advmat.de

- [37] H. Jin, P. Li, P. Cui, J. Shi, W. Zhou, X. Yu, W. Song, C. Cao, Nat. Commun. 2022, 13, 723.
- [38] H. Li, L. Fang, T. Wang, R. Bai, J. Zhang, T. Li, Z. Duan, K.-J. Chen, F. Pan, Adv. Mater. 2025, 37, 2416337.
- [39] T. Moragues, G. Giannakakis, A. Ruiz-Ferrando, C. N. Borca, T. Huthwelker, A. Bugaev, A. J. de Mello, J. Pérez-Ramírez, S. Mitchell, Angew. Chem., Int. Ed. 2024, 63, 202401056.
- [40] J. Guo, Y. Haghshenas, Y. Jiao, P. Kumar, B. I. Yakobson, A. Roy, Y. Jiao, K. Regenauer-Lieb, D. Nguyen, Z. Xia, Adv. Mater. 2024, 36, 2407102.
- [41] S. T. Stripp, B. R. Duffus, V. Fourmond, C. Léger, S. Leimkühler, S. Hirota, Y. Hu, A. Jasniewski, H. Ogata, M. W. Ribbe, *Chem. Rev.* 2022, 122. 11900.
- [42] B. Ginovska, O. Y. Gutiérrez, A. Karkamkar, M.-S. Lee, J. A. Lercher, Y. Liu, S. Raugei, R. Rousseau, W. J. Shaw, ACS Catal. 2023, 13, 11883.
- [43] L. Ma, Y. Wang, Y. Chen, R. Han, D. Xu, D. Jiao, D. Wang, X. Yang, Adv. Funct. Mater. 2025, 2503358.
- [44] S. K. Kaiser, Z. Chen, D. Faust Akl, S. Mitchell, J. Pérez-Ramírez, Chem. Rev. 2020, 120, 11703.
- [45] A. J. Medford, A. Vojvodic, J. S. Hummelshøj, J. Voss, F. Abild-Pedersen, F. Studt, T. Bligaard, A. Nilsson, J. K. Nørskov, J. Catal. 2015, 328, 36.
- [46] L. Li, X. Dai, M. Lu, C. Guo, S. M. Wabaidur, X.-L. Wu, Z. Lou, Y. Zhong, Y. Hu, Adv. Powder Mater. 2024, 3, 100170.
- [47] F. Kong, Y. Huang, X. Yu, M. Li, K. Song, Q. Guo, X. Cui, J. Shi, J. Am. Chem. Soc. 2024, 146, 30078.
- [48] F. Zhang, Y. Zhu, Q. Lin, L. Zhang, X. Zhang, H. Wang, Energy Environ. Sci. 2021, 14, 2954.
- [49] X. Li, H. Lei, L. Xie, N. Wang, W. Zhang, R. Cao, Acc. Chem. Res. 2022, 55, 878.
- [50] X. Huang, J. T. Groves, Chem. Rev. 2018, 118, 2491.
- [51] A. Kumar, S. Ibraheem, T. Anh Nguyen, R. K. Gupta, T. Maiyalagan, G. Yasin, Coord. Chem. Rev. 2021, 446, 214122.
- [52] W. Zhang, W. Lai, R. Cao, Chem. Rev. 2017, 117, 3717.
- [53] S. Yang, Y. Yu, X. Gao, Z. Zhang, F. Wang, Chem. Soc. Rev. 2021, 50, 12985
- [54] Y. Li, N. Wang, H. Lei, X. Li, H. Zheng, H. Wang, W. Zhang, R. Cao, Coord. Chem. Rev. 2021, 442, 213996.
- [55] S. Ren, D. Joulié, D. Salvatore, K. Torbensen, M. Wang, M. Robert, C. P. Berlinguette, *Science* 2019, 365, 367.
- [56] X. Zhang, Y. Wang, M. Gu, M. Wang, Z. Zhang, W. Pan, Z. Jiang, H. Zheng, M. Lucero, H. Wang, G. E. Sterbinsky, Q. Ma, Y.-G. Wang, Z. Feng, J. Li, H. Dai, Y. Liang, Nat. Energy 2020, 5, 684.
- [57] Y. Wu, Z. Jiang, X. Lu, Y. Liang, H. Wang, Nature 2019, 575, 639.
- [58] X. Wang, Q. Li, Z. Zhao, L. Yu, S. Wang, H. Pu, M. Adeli, L. Qiu, P. Gu, L. Li, C. Cheng, Adv. Funct. Mater. 2024, 34, 2313143.
- [59] X. Lu, L. Kuai, F. Huang, J. Jiang, J. Song, Y. Liu, S. Chen, L. Mao, W. Peng, Y. Luo, Y. Li, H. Dong, B. Li, J. Shi, *Nat. Commun.* 2023, 14, 6767.
- [60] S. Liu, D. Liu, Y. Sun, P. Xiao, H. Lin, J. Chen, X.-L. Wu, X. Duan, S. Wang, Appl. Catal., B 2022, 310, 121327.
- [61] J. Yang, R. Zhang, H. Zhao, H. Qi, J. Li, J.-F. Li, X. Zhou, A. Wang, K. Fan, X. Yan, T. Zhang, Exploration 2022, 2, 20210267.
- [62] P. Makam, S. S. R. K. C. Yamijala, V. S. Bhadram, L. J. W. Shimon, B. M. Wong, E. Gazit, Nat. Commun. 2022, 13, 1505.
- [63] J. Wang, K. Wang, F.-B. Wang, X.-H. Xia, Nat. Commun. 2014, 5, 5285.
- [64] L. Li, W. Liu, H. Ying, X. He, S. Shang, P. Zhang, X. Zhang, S. Liu, H. Wang, Y. Xie, CCS Chem. 2024, 6, 3077.
- [65] Y. Yang, K. Mao, S. Gao, H. Huang, G. Xia, Z. Lin, P. Jiang, C. Wang, H. Wang, Q. Chen, Adv. Mater. 2018, 30, 1801732.
- [66] R. Fu, J. guo, H. Jin, Z. Li, J. Xia, Y. Tang, Y. Ding, H. Zhao, D. Ye, J. Xu, Small 2025, 21, 2409113.

- [67] Y. Wang, G. Jia, X. Cui, X. Zhao, Q. Zhang, L. Gu, L. Zheng, L. H. Li, Q. Wu, D. J. Singh, D. Matsumura, T. Tsuji, Y.-T. Cui, J. Zhao, W. Zheng, Chem 2021, 7, 436.
- [68] Y. Wang, A. Cho, G. Jia, X. Cui, J. Shin, I. Nam, K.-J. Noh, B. J. Park, R. Huang, J. W. Han, Angew. Chem., Int. Ed. 2023, 62, 202300119.
- [69] J. Wu, X. Zhu, Q. Li, Q. Fu, B. Wang, B. Li, S. Wang, Q. Chang, H. Xiang, C. Ye, Q. Li, L. Huang, Y. Liang, D. Wang, Y. Zhao, Y. Li, Nat. Commun. 2024, 15, 6174.
- [70] D. Chen, Z. Xia, Z. Guo, W. Gou, J. Zhao, X. Zhou, X. Tan, W. Li, S. Zhao, Z. Tian, Y. Qu, Nat. Commun. 2023, 14, 7127.
- [71] L. Zhang, N. Jin, Y. Yang, X.-Y. Miao, H. Wang, J. Luo, L. Han, Nano-Micro Lett. 2023, 15, 228.
- [72] L. Huang, J. Chen, L. Gan, J. Wang, S. Dong, Sci. Adv. 2019, 5, aav5490.
- [73] W. Xu, Y. Wu, X. Wang, Y. Qin, H. Wang, Z. Luo, J. Wen, L. Hu, W. Gu, C. Zhu, Angew. Chem., Int. Ed. 2023, 62, 202304625.
- [74] W. Liu, L. Zhang, X. Liu, X. Liu, X. Yang, S. Miao, W. Wang, A. Wang, T. Zhang, J. Am. Chem. Soc. 2017, 139, 10790.
- [75] A. Wang, J. Li, T. Zhang, Nat. Rev. Chem. 2018, 2, 65.
- [76] J.-R. Huang, X.-F. Qiu, Z.-H. Zhao, H.-L. Zhu, Y.-C. Liu, W. Shi, P.-Q. Liao, X.-M. Chen, Angew. Chem., Int. Ed. 2022, 61, 202210985.
- [77] Z. Qi, Y. Zhou, R. Guan, Y. Fu, J.-B. Baek, Adv. Mater. 2023, 35, 2210575.
- [78] C. Jacob, G. I. Giles, N. M. Giles, H. Sies, Angew. Chem., Int. Ed. 2003, 42, 4742.
- [79] H.-Y. Tan, S.-C. Lin, J. Wang, C.-J. Chang, S.-C. Haw, K.-H. Lin, L. D. Tsai, H.-C. Chen, H. M. Chen, ACS Appl. Mater. Interfaces 2021, 13, 52134.
- [80] Z. Jin, D. Jiao, Y. Dong, L. Liu, J. Fan, M. Gong, X. Ma, Y. Wang, W. Zhang, L. Zhang, Z. Gen Yu, D. Voiry, W. Zheng, X. Cui, Angew. Chem., Int. Ed. 2024, 63, 202318246.
- [81] J. Wang, H. Li, S. Liu, Y. Hu, J. Zhang, M. Xia, Y. Hou, J. Tse, J. Zhang, Y. Zhao, Angew. Chem., Int. Ed. 2021, 60, 181.
- [82] J. Deng, A. Walther, Adv. Mater. 2020, 32, 2002629.
- [83] S. Ji, B. Jiang, H. Hao, Y. Chen, J. Dong, Y. Mao, Z. Zhang, R. Gao, W. Chen, R. Zhang, Q. Liang, H. Li, S. Liu, Y. Wang, Q. Zhang, L. Gu, D. Duan, M. Liang, D. Wang, X. Yan, Y. Li, Nat. Catal. 2021, 4, 407.
- [84] K. Yuan, D. Lützenkirchen-Hecht, L. Li, L. Shuai, Y. Li, R. Cao, M. Qiu, X. Zhuang, M. K. H. Leung, Y. Chen, U. Scherf, J. Am. Chem. Soc. 2020, 142, 2404.
- [85] J. Wan, Z. Zhao, H. Shang, B. Peng, W. Chen, J. Pei, L. Zheng, J. Dong, R. Cao, R. Sarangi, Z. Jiang, D. Zhou, Z. Zhuang, J. Zhang, D. Wang, Y. Li, J. Am. Chem. Soc. 2020, 142, 8431.
- [86] S. Zhang, X. J. Gao, Y. Ma, K. Song, M. Ge, S. Ma, L. Zhang, Y. Yuan, W. Jiang, Z. Wu, L. Gao, X. Yan, B. Jiang, *Nat. Commun.* 2024, 15, 10605.
- [87] C. Gu, Y. Zhang, P. He, M. Gan, J. Zhu, H. Yin, J. Hazard. Mater. 2024, 472, 134515.
- [88] J.-X. Peng, W. Yang, Z. Jia, L. Jiao, H.-L. Jiang, Nano Res. 2022, 15, 10063.
- [89] W. Ni, H. Chen, J. Zeng, Y. Zhang, H. A. Younus, Z. Zeng, M. Dai, W. Zhang, S. Zhang, Energy Environ. Sci. 2023, 16, 3679.
- [90] Y. Min, X. Zhou, J.-J. Chen, W. Chen, F. Zhou, Z. Wang, J. Yang, C. Xiong, Y. Wang, F. Li, H.-Q. Yu, Y. Wu, Nat. Commun. 2021, 12, 303.
- [91] K. Wang, Q. Hong, C. Zhu, Y. Xu, W. Li, Y. Wang, W. Chen, X. Gu, X. Chen, Y. Fang, Y. Shen, S. Liu, Y. Zhang, *Nat. Commun.* 2024, 15, 5705.
- [92] Y. Jung, C. W. Lee, B.-H. Lee, Y. Yu, J. Moon, H. S. Lee, W. Ko, J. Bok, K. Lee, J. Lee, M. S. Bootharaju, J. Ryu, M. Kim, T. Hyeon, J. Am. Chem. Soc. 2025, 147, 1740.
- [93] X. Yuan, X. Wu, J. Xiong, B. Yan, R. Gao, S. Liu, M. Zong, J. Ge, W. Lou, Nat. Commun. 2023, 14, 5974.
- [94] Y. Wang, B. J. Park, V. K. Paidi, R. Huang, Y. Lee, K.-J. Noh, K.-S. Lee, J. W. Han, ACS Energy Lett. 2022, 7, 640.

and Conditions (https://onlinelibrary.wiley

conditions) on Wiley Online Library for rules of use; OA articles are governed by the applicable Creative Commons L

www.advmat.de

- [95] J. Shan, C. Ye, Y. Jiang, M. Jaroniec, Y. Zheng, S.-Z. Qiao, Sci. Adv. 2022, 8, abo0762.
- [96] Y. Gao, B. Liu, D. Wang, Adv. Mater. 2023, 35, 2209654.
- [97] G. Jia, Y. Zhang, J. C. Yu, Z. Guo, Adv. Mater. 2024, 36, 2403153.
- [98] M. Liu, X. Wang, S. Cao, X. Lu, W. Li, N. Li, X.-H. Bu, Adv. Mater. 2024, 36, 2309231.
- [99] Z. Li, D. Wu, Q. Wang, Q. Zhang, P. Xu, F. Liu, S. Xi, D. Ma, Y. Lu, L. Jiang, Z. Zhang, Adv. Mater. 2024, 36, 2408364.
- [100] L. Jiao, N. Tao, Y. Kang, W. Song, Y. Chen, Y. Zhang, W. Xu, Y. Wu, W. Gu, L. Zheng, L. Chen, L. Deng, C. Zhu, Y.-N. Liu, *Nano Today* 2023, 50, 101859
- [101] C. K. T. Wun, H. K. Mok, T. Chen, T.-S. Wu, K. Taniya, K. Nakagawa, S. Day, C. C. Tang, Z. Huang, H. Su, W.-Y. Yu, T. K. W. Lee, T. W. B. Lo, Chem. Catal. 2022, 2, 2346.
- [102] J. Li, H. Huang, W. Xue, K. Sun, X. Song, C. Wu, L. Nie, Y. Li, C. Liu, Y. Pan, H.-L. Jiang, D. Mei, C. Zhong, Nat. Catal. 2021, 4, 719.
- [103] G. Schwarz, R. R. Mendel, M. W. Ribbe, Nature 2009, 460, 839.
- [104] N. Rouhier, Nat. Chem. Biol. 2023, 19, 129.
- [105] X. Liang, N. Fu, S. Yao, Z. Li, Y. Li, J. Am. Chem. Soc. 2022, 144, 18155.
- [106] S. Sultan, J. N. Tiwari, A. N. Singh, S. Zhumagali, M. Ha, C. W. Myung, P. Thangavel, K. S. Kim, Adv. Energy Mater. 2019, 9, 1900624.
- [107] X. Li, S. Mitchell, Y. Fang, J. Li, J. Perez-Ramirez, J. Lu, Nat. Rev. Chem. 2023, 7, 754.
- [108] J. Xi, R. Zhang, L. Wang, W. Xu, Q. Liang, J. Li, J. Jiang, Y. Yang, X. Yan, K. Fan, L. Gao, Adv. Funct. Mater. 2021, 31, 2007130.
- [109] J. Xia, J. Xu, B. Yu, X. Liang, Z. Qiu, H. Li, H. Feng, Y. Li, Y. Cai, H. Wei, H. Li, H. Xiang, Z. Zhuang, D. Wang, Angew. Chem., Int. Ed. 2024, 63, 202412740.
- [110] B. Yang, H. Yao, J. Yang, C. Chen, J. Shi, Nat. Commun. 2022, 13, 1988.
- [111] L. Gloag, S. V. Somerville, J. J. Gooding, R. D. Tilley, Nat. Rev. Mater. 2024, 9, 173.
- [112] D. Leybo, U. J. Etim, M. Monai, S. R. Bare, Z. Zhong, C. Vogt, Chem. Soc. Rev. 2024, 53, 10450.
- [113] K. Qi, M. Chhowalla, D. Voiry, Mater. Today 2020, 40, 173.
- [114] Y. Tang, X. Liu, P. Qi, Y. Cai, H. Wang, Y. Qin, W. Gu, C. Wang, Y. Sun, C. Zhu, ACS Nano 2024, 18, 25685.
- [115] R. M. Garrett, J. L. Johnson, T. N. Graf, A. Feigenbaum, K. V. Rajagopalan, Proc. Natl. Acad. Sci. 1998, 95, 6394.
- [116] L.-Z. Huang, X. Wei, E. Gao, C. Zhang, X.-M. Hu, Y. Chen, Z. Liu, N. Finck, J. Lützenkirchen, D. D. Dionysiou, Appl. Catal., B 2020, 268, 118459
- [117] S. Jena, J. Dutta, K. D. Tulsiyan, A. K. Sahu, S. S. Choudhury, H. S. Biswal, *Chem. Soc. Rev.* **2022**, *51*, 4261.
- [118] J.-B. Liu, H.-S. Gong, G.-L. Ye, H.-L. Fei, Rare Met. 2022, 41, 1703.
- [119] Z.-S. Zhu, S. Zhong, C. Cheng, H. Zhou, H. Sun, X. Duan, S. Wang, Chem. Rev. 2024, 124, 11348.
- [120] C. D. Ma, C. Wang, C. Acevedo-Vélez, S. H. Gellman, N. L. Abbott, Nature 2015, 517, 347.
- [121] C. Xu, C. Guo, J. Liu, B. Hu, H. Chen, G. Li, X. Xu, C. Shu, H. Li, C. Chen, Small 2023, 19, 2207675.
- [122] R. Pan, Q. Wang, Y. Zhao, Z. Feng, Y. Xu, Z. Wang, Y. Li, X. Zhang, H. Zhang, J. Liu, X.-K. Gu, J. Zhang, Y. Weng, J. Zhang, Sci. Adv. 2024, 10, adq2791.
- [123] J. Sui, M.-L. Gao, B. Qian, C. Liu, Y. Pan, Z. Meng, D. Yuan, H.-L. Jiang, Sci. Bull. 2023, 68, 1886.
- [124] B. Yu, Y. Zhao, G. Li, R. Deng, R. Liu, L. Zhang, W. Wang, W. Liu, B. Qiao, CCS Chem. 2025, https://doi.org/10.31635/ccschem.024. 202404694.
- [125] S.-O. Shan, S. Loh, D. Herschlag, Science 1996, 272, 97.
- [126] Y.-H. Wang, S. Zheng, W.-M. Yang, R.-Y. Zhou, Q.-F. He, P. Radjenovic, J.-C. Dong, S. Li, J. Zheng, Z.-L. Yang, G. Attard, F. Pan, Z.-Q. Tian, J.-F. Li, *Nature* 2021, 600, 81.

- [127] Q. Sun, N. J. Oliveira, S. Kwon, S. Tyukhtenko, J. J. Guo, N. Myrthil, S. A. Lopez, I. Kendrick, S. Mukerjee, L. Ma, S. N. Ehrlich, J. Li, W. A. Goddard, Y. Yan, Q. Jia, Nat. Energy 2023, 8, 859.
- [128] P. Li, Y. Jiang, Y. Hu, Y. Men, Y. Liu, W. Cai, S. Chen, Nat. Catal. 2022, 5, 900.
- [129] X. Zhao, Y. Liu, J. Am. Chem. Soc. 2020, 142, 5773.
- [130] J. Cui, X. Gao, K. Pang, W. Wu, M. K. Awasthi, Y. Zhao, X. Yin, Sep. Purif. Technol. 2025, 361, 131365.
- [131] C. H. Sharp, B. C. Bukowski, H. Li, E. M. Johnson, S. Ilic, A. J. Morris, D. Gersappe, R. Q. Snurr, J. R. Morris, *Chem. Soc. Rev.* **2021**, *50*, 11530.
- [132] M. E. Davis, Nature 2002, 417, 813.
- [133] R. Zhu, Z. Zhao, R. Yan, M. Wu, W. Zheng, M. Wang, C. Cheng, S. Li, C. Zhao, Adv. Funct. Mater. 2024, 34, 2314593.
- [134] L. Ni, C. Yu, Q. Wei, D. Liu, J. Qiu, Angew. Chem., Int. Ed. 2022, 61, 202115885.
- [135] G. Cai, P. Yan, L. Zhang, H.-C. Zhou, H.-L. Jiang, Chem. Rev. 2021, 121, 12278.
- [136] Y. Ma, H. Li, J. Liu, D. Zhao, Nat. Rev. Chem. 2024, 8, 915.
- [137] R. Yan, Z. Zhao, R. Zhu, M. Wu, X. Liu, M. Adeli, B. Yin, C. Cheng, S. Li, Angew. Chem., Int. Ed. 2024, 63, 202404019.
- [138] K. Cheng, Z. Liu, D. Jiang, M. Song, Y. Wang, Nano Res. 2024, 17, 2352.
- [139] Y. Chen, Y. Wu, L. Li, Y. Liao, S. Luo, H. Xu, Y. Wu, Y. Qing, Chem. Eng. J. 2023, 475, 145993.
- [140] M. Peng, C. Li, Z. Wang, M. Wang, Q. Zhang, B. Xu, M. Li, D. Ma, Chem. Rev. 2025, 125, 2371.
- [141] P. R. D. Murray, J. H. Cox, N. D. Chiappini, C. B. Roos, E. A. McLoughlin, B. G. Hejna, S. T. Nguyen, H. H. Ripberger, J. M. Ganley, E. Tsui, N. Y. Shin, B. Koronkiewicz, G. Qiu, R. R. Knowles, Chem. Rev. 2022, 122, 2017.
- [142] Q. Zhao, Q. Zhang, Y. Xu, A. Han, H. He, H. Zheng, W. Zhang, H. Lei, U.-P. Apfel, R. Cao, Angew. Chem., Int. Ed. 2024, 63, 202414104.
- [143] Y. Tang, X. Liu, P. Qi, W. Xu, Y. Wu, Y. Cai, W. Gu, H. Sun, C. Wang, C. Zhu. Nano Lett. 2024. 24. 9974.
- [144] Y. Wu, H. Zhong, W. Xu, R. Su, Y. Qin, Y. Qiu, L. Zheng, W. Gu, L. Hu, F. Lv, S. Zhang, S. P. Beckman, Y. Lin, C. Zhu, S. Guo, Angew. Chem., Int. Ed. 2024, 63, 202319108.
- [145] Y. Lyu, P. Scrimin, ACS Catal. 2021, 11, 11501.
- [146] M. D. Wodrich, X. Hu, Nat. Rev. Chem. 2017, 2, 0099.
- [147] M. Frey, ChemBioChem 2002, 3, 153.
- [148] T. R. Simmons, G. Berggren, M. Bacchi, M. Fontecave, V. Artero, Coord. Chem. Rev. 2014, 270, 127.
- [149] C. Tard, C. J. Pickett, Chem. Rev. 2009, 109, 2245.
- [150] A. Pardo, A. L. De Lacey, V. M. Fernández, H.-J. Fan, Y. Fan, M. B. Hall, J. Biol. Inorg. Chem. 2006, 11, 286.
- [151] B.-H. Lee, S. Park, M. Kim, A. K. Sinha, S. C. Lee, E. Jung, W. J. Chang, K.-S. Lee, J. H. Kim, S.-P. Cho, H. Kim, K. T. Nam, T. Hyeon, *Nat. Mater.* 2019, 18, 620.
- [152] G. Yang, D. Wang, Y. Wang, W. Hu, S. Hu, J. Jiang, J. Huang, H.-L. Jiang, J. Am. Chem. Soc. 2024, 146, 10798.
- [153] S. Hu, M.-L. Gao, J. Huang, H. Wang, Q. Wang, W. Yang, Z. Sun, X. Zheng, H.-L. Jiang, J. Am. Chem. Soc. 2024, 146, 20391.
- [154] C. Yang, Z. Wu, Y. Zheng, Y. Gao, T. Ma, Z. Zeng, Y. Wang, C. Cheng, S. Li, Adv. Funct. Mater. 2024, 34, 2404061.
- [155] S. Xu, Y. Ding, J. Du, Y. Zhu, G. Liu, Z. Wen, X. Liu, Y. Shi, H. Gao, L. Sun, F. Li, ACS Catal. 2022, 12, 5502.
- [156] M. I. Ahmed, L. J. Arachchige, Z. Su, D. B. Hibbert, C. Sun, C. Zhao, ACS Catal. 2022, 12, 1443.
- [157] J. Chen, Q. Ma, X. Zheng, Y. Fang, J. Wang, S. Dong, Nat. Commun. 2022, 13, 2808.
- [158] R. Zhang, X. Yan, K. Fan, Acc. Mater. Res. 2021, 2, 534.
- [159] M. R. A. Blomberg, Chem. Soc. Rev. 2020, 49, 7301.
- [160] M. R. A. Blomberg, J. Inorg. Biochem. 2020, 203, 110866.

from https://advanced.onlinelibrary.wiley.com/doi/10.1002/adma.202502131 by HONG KONG POLYTECHNIC UNIVERSITY HU NG HOM, Wiley Online Library on [28/09/2025]. See the Terms

and-conditions) on Wiley Online Library for rules of use; OA articles are governed by the applicable Creative Common



#### www.advancedsciencenews.com

- [161] I. Ishigami, R. G. Sierra, Z. Su, A. Peck, C. Wang, F. Poitevin, S. Lisova, B. Hayes, F. R. Moss, S. Boutet, R. E. Sublett, C. H. Yoon, S.-R. Yeh, D. L. Rousseau, *Nat. Commun.* 2023, 14, 5752.
- [162] C. J. Reed, Q. N. Lam, E. N. Mirts, Y. Lu, Chem. Soc. Rev. 2021, 50, 2486
- [163] X. Lu, S. Gao, H. Lin, H. Tian, D. Xu, J. Shi, Natl. Sci. Rev. 2022, 9, nwac022.
- [164] H. Zou, S. Shu, W. Yang, Y.-c. Chu, M. Cheng, H. Dong, H. Liu, F. Li, J. Hu, Z. Wang, W. Liu, H. M. Chen, L. Duan, *Nat. Commun.* 2024, 15, 10818.
- [165] Y.-T. Xi, P.-J. Wei, R.-C. Wang, J.-G. Liu, Chem. Commun. 2015, 51, 7455.
- [166] Y. Wang, P. Zhang, X. Xu, W.-S. Yu, Z. Duan, H. Huang, T. Wang, G. Fu, Z. Zhou, S. Sun, Angew. Chem., Int. Ed. 2025, 64, 202418897.
- [167] T. Tsukihara, H. Aoyama, E. Yamashita, T. Tomizaki, H. Yamaguchi, K. Shinzawa-Itoh, R. Nakashima, R. Yaono, S. Yoshikawa, *Science* 1995, 269, 1069.
- [168] R. Hille, J. Hall, P. Basu, Chem. Rev. 2014, 114, 3963.

- [169] L. Jiao, J. Zhu, Y. Zhang, W. Yang, S. Zhou, A. Li, C. Xie, X. Zheng, W. Zhou, S.-H. Yu, H.-L. Jiang, J. Am. Chem. Soc. 2021, 143, 19417.
- [170] Z.-X. Pan, S. Yang, X. Chen, J.-X. Luo, R.-Z. Zhang, P. Yang, Q. Xu, J.-Y. Yue, Chem. Eng. J. 2024, 493, 152798.
- [171] Y. Zhou, S. Liu, Y. Gu, G.-H. Wen, J. Ma, J.-L. Zuo, M. Ding, J. Am. Chem. Soc. 2021, 143, 14071.
- [172] M. Sun, B. Huang, Adv. Energy Mater. 2023, 13, 2301948.
- [173] M. Sun, B. Huang, Adv. Energy Mater. 2024, 14, 2400152.
- [174] L. Cheng, Y. Tang, K. Ostrikov, Q. Xiang, Angew. Chem., Int. Ed. 2024, 63, 202313599.
- [175] B. M. Hoffman, D. Lukoyanov, D. R. Dean, L. C. Seefeldt, Acc. Chem. Res. 2013, 46, 587.
- [176] M. Xi, H. Zhang, L. Yang, Y. Long, Y. Zhao, A. Chen, Q. Xiao, T. Liu, X. Xiao, G. Hu, Adv. Sci. 2025, 12, 2409855.
- [177] Y. Sun, Y. Zang, B. He, G. Lin, Z. Liu, L. Yang, L. Chen, L. Li, X. Liu, C. Shen, H. Qiu, *Sci. Adv.* **2025**, *11*, adq2948.
- [178] Z. Lang, X. Wang, S. Jabeen, Y. Cheng, N. Liu, Z. Liu, T. Gan, Z. Zhuang, H. Li, D. Wang, Adv. Mater. 2025, 37, 2418942.



Ying Wang is currently an associate professor in the College of Materials Science and Chemical Engineering of the Harbin Engineering University. She worked as a research fellow under the supervision of Prof. Kwok-Yin Wong at the Department of Applied Biology and Chemical Technology, The Hong Kong Polytechnic University from 2021 to 2024. She is interested in the design and synthesis of single-atom sites for energy conversion and bioapplication.



**Guangri Jia** is currently a post-doctoral fellow under the supervision of Prof. Zhengxiao Guo at the Department of Chemistry, The University of Hong Kong. He received his Ph.D. degree from Jilin University, China, in 2021. From 2021 to 2023, he worked as a research assistant in Prof. Jimmy Yu's group at The Chinese University of Hong Kong. His research interests focus on single-atom heterogeneous catalysts for photocatalytic energy conversion.



**Piaoping Yang** received his B.S. degree from the Department of Chemistry from Jilin University in 2002 and his Ph.D. from the Department of Chemistry at Jilin University in 2005. He joined the College of Materials Science and Chemical Engineering of the Harbin Engineering University in 2005. His research interests focus on energy materials, biomedical materials, and rare earth-based functional materials.

15214095, 0, Downloaded from https://advanced.onlinelibrary.wiley.com/doi/10.1002/adma.02502131 by HONG KONG POLYTECHNIC UNIVERSITY HU NG HOM, Wiley Online Library on [28.092025]. See the Terms

and-conditions) on Wiley Online Library for rules of use; OA articles are governed by the applicable Creative Commons License



**Linshan Zhang** is currently a post-doctoral fellow under the supervision of Prof. Kwok-Yin Wong at the Department of Applied Biology and Chemical Technology, The Hong Kong Polytechnic University. She received her Ph.D. degree from the College of Biomass Science and Engineering, Sichuan University, in 2022 under the supervision of Prof. Luming Yang. She is interested in the design of nanomaterials for environmental pollutant treatments.



**Kwok-Yin Wong** received his BSc and Ph.D. degrees from the Department of Chemistry, The University of Hong Kong and was a postdoctoral research fellow at the Division of Chemistry and Chemical Engineering of California Institute of Technology, U.S.A. He is now the Patrick S.C. Poon Endowed Professor of Applied Chemistry and Chair Professor of Chemical Technology in the Department of Applied Biology and Chemical Technology of the Hong Kong Polytechnic University. His research interests include biosensors for antibiotics and the application of nanomaterials as catalysts for green chemistry.